Modular kinetic analysis

To investigate differences in oxidative phosphorylation caused by PINK1 knock-out, we applied a systems approach, namely modular kinetic analysis (Amo and Brand, 2007; Brand, 1990). This analyzes the kinetics of the whole of oxidative phosphorylation divided into three modules connected by their common substrate or product, $\Delta\psi$. The modules are (i) the reactions that produce $\Delta\psi$, consisting of the substrate translocases, dehydrogenases and other enzymes and the components of the respiratory chain, called 'substrate oxidation'; (ii) the reactions that consume $\Delta\psi$ and synthesize, export and dephosphorylate ATP, consisting of ATP synthase, the phosphate and adenine nucleotide translocases and any ATPases that may be present, called the 'phosphorylating system'; and (iii) the reactions that consume $\Delta\psi$ without ATP synthesis, called the 'proton leak' (Brand, 1990). The analysis reports changes anywhere within oxidative phosphorylation that are functionally important but is unresponsive to changes that have no functional consequences. Comparison of the kinetic responses of each of the three modules to $\Delta\psi$ obtained using mitochondria isolated from PINK1$^{+/+}$ and PINK1$^{-/-}$ MEFs would reveal any effects of PINK1 on the kinetics of oxidative phosphorylation. Oxygen consumption and $\Delta\psi$ were measured simultaneously using mitochondria incubated with 80 ng/ml nigericin and 4 μM rotenone. Respiration was initiated by 5 mM succinate. The kinetic behavior of a '$\Delta\psi$-producer' can be established by specific modulation of a $\Delta\psi$-consumer and the kinetics of a consumer can be established by specific modulation of a $\Delta\psi$-producer (Brand, 1998). To measure the kinetic response of proton leak to $\Delta\psi$, the State 4 (non-phosphorylating) respiration of mitochondria in the presence of oligomycin (0.8 μg/ml; to prevent any residual ATP synthesis), which was used solely to drive the proton leak, was titrated with malonate (up to 8 mM). In a similar way, State 4 respiration was titrated by FCCP (up to 1 μM) for measurement of the kinetic response of substrate oxidation to $\Delta\psi$. State 3 (maximal rate of ATP synthesis) was obtained by addition of excess ADP (1 mM). Titration of State 3 respiration with malonate (up to 1.1 mM) allowed measurement of the kinetics of the $\Delta\psi$-consumers (the sum of the phosphorylating system and proton leak). The coupling efficiencies of oxidative phosphorylation were calculated from the kinetic curves as the percentage of mitochondrial respiration rate at a given $\Delta\psi$ that was used for ATP synthesis and was therefore inhibited by oligomycin. Note that any slip reactions will appear as proton leak in this analysis (Brand et al., 1994).

Mitochondrial ROS production

Mitochondrial ROS production rate was assessed by measurement of H_2O_2 generation rate, determined fluorometrically by measurement of oxidation of Amplex Red to fluorescent resorufin coupled to the enzymatic reduction of H_2O_2 by horseradish peroxidase using a spectrofluorometer RF-5300PC (Shimadzu, Kyoto, Japan). The H_2O_2 generation rate was measured in non-phosphorylating conditions (=State 4) using either pyruvate/malate or succinate as respiratory substrates. Mitochondria were incubated at 0.1 mg/ml in respiration buffer. All incubations also contained 5 μM Amplex Red, 2 U/ml horseradish peroxidase and 8 U/ml superoxide dismutase. The reaction was initiated by addition of 5 mM succinate or 4 mM pyruvate + 1 mM malonate and the increase in fluorescence was followed at excitation and emission wavelengths of 560 and 590 nm, respectively. Appropriate correction for background signals and standard curves generated using known amounts of H_2O_2 were used to calculate the rate of H_2O_2 production in nmol/min/mg mitochondrial protein. The percentage free radical leak, which is a measure of the number of electrons that produce superoxide (and subsequently H_2O_2) compared with the total number of electrons which pass thorough the respiratory chain, was calculated as the rate of H_2O_2 production divided by the rate of O_2 consumption (Barja et al., 1994).

Statistics

Values are presented as means ± SEM except Fig. 2D, in which error bars indicate SD. The significance of differences between means was assessed by the unpaired Student's *t*-test using Microsoft Excel; *P* values <0.05 were taken to be significant.

Results

Cell growth and mitochondrial morphology

In general, cultured cells gain their energy mostly from glycolysis. Therefore, cells deficient in respiratory function can grow in normal medium, although possibly at a slower rate, relying predominantly on glycolysis (Hofhaus et al., 1996). Actually, ρ^0 cells, which lack mitochondrial DNA completely, can grow producing energy exclusively through glycolysis (King and Attardi, 1989). On the other hand, galactose metabolism via glycolysis is much slower than glucose metabolism (Reitzer et al., 1979). Therefore, cells in galactose medium are forced to oxidize pyruvate through the mitochondrial respiratory chain for energy required for growth. Consequently, cells with defects in their mitochondrial respiratory chains show growth impairments in galactose medium. To evaluate this phenomenon is also observed in our cells, we examined growth retardation by addition of mitochondrial complex I inhibitor, rotenone (Fig. 1A). In glucose medium, 10 nM rotenone had only a slight effect on the growth of PINK1$^{+/+}$ MEFs and slower growth was observed even in the presence of 100 nM rotenone. However, in the galactose medium, 10 nM rotenone significantly inhibited the growth of PINK1$^{+/+}$ MEFs and 100 nM roteone completely arrested the growth. Therefore, we could confirm that the growth impairment of our cells in the galactose medium was due to mitochondrial respiratory chain defects.

PINK1 acts upstream of parkin, regulating mitochondrial integrity and function; therefore, loss of PINK1 is considered to affect mitochondrial functions. To assess the mitochondrial functions of PINK1$^{-/-}$ MEFs, growth capability in a medium in which galactose replaced glucose was examined. As shown in Fig. 1B, PINK1$^{-/-}$ MEFs appeared to show clear growth impairments in the galactose medium, whereas PINK1$^{+/+}$ MEFs grew slightly slower than in the glucose medium.

No differences of mitochondrial morphology between PINK1$^{+/+}$ and $^{-/-}$ MEFs in the glucose medium were detected (Fig. 1C), consistent with the previous report (Matsuda et al., 2010). However, in the galactose medium, mitochondria of the PINK1$^{-/-}$ MEFs were more fragmented compared to the PINK$^{+/+}$ MEFs (Fig. 1C). This is consistent with previous reports, which found mitochondrial morphological changes were more pronounced when PINK1 knock-down HeLa cells were grown in low-glucose medium (Exner et al., 2007) and human PINK1 homozygous mutant fibroblast in galactose medium (Grünewald et al., 2009). In these cells, mitochondrial morphological changes were associated with the mitochondrial functional impairment.

Assessments of mitochondrial functions at the cellular level

Because PINK1$^{-/-}$ MEFs showed severe growth impairments in the galactose medium, the mitochondrial functions of these cells were assessed at the cellular level. First, cellular respiration rates were measured (Fig. 2A). The basal respiration rate was significantly reduced in PINK1$^{-/-}$ cells compared with that in PINK1$^{+/+}$ cells (11.13 ± 0.71 versus 14.36 ± 1.01 nmol O/min/10^6 cells; $p<0.05$; $n=5$ independent experiments), consistent with previous reports using partial knock-down of PINK1 expression (Gandhi et al., 2009; Liu et al., 2009). Oligomycin inhibits ATP synthase, resulting in non-phosphorylating respiration. FCCP uncouples oxidative phosphorylation, leading to maximum respiration rates. In both conditions, the

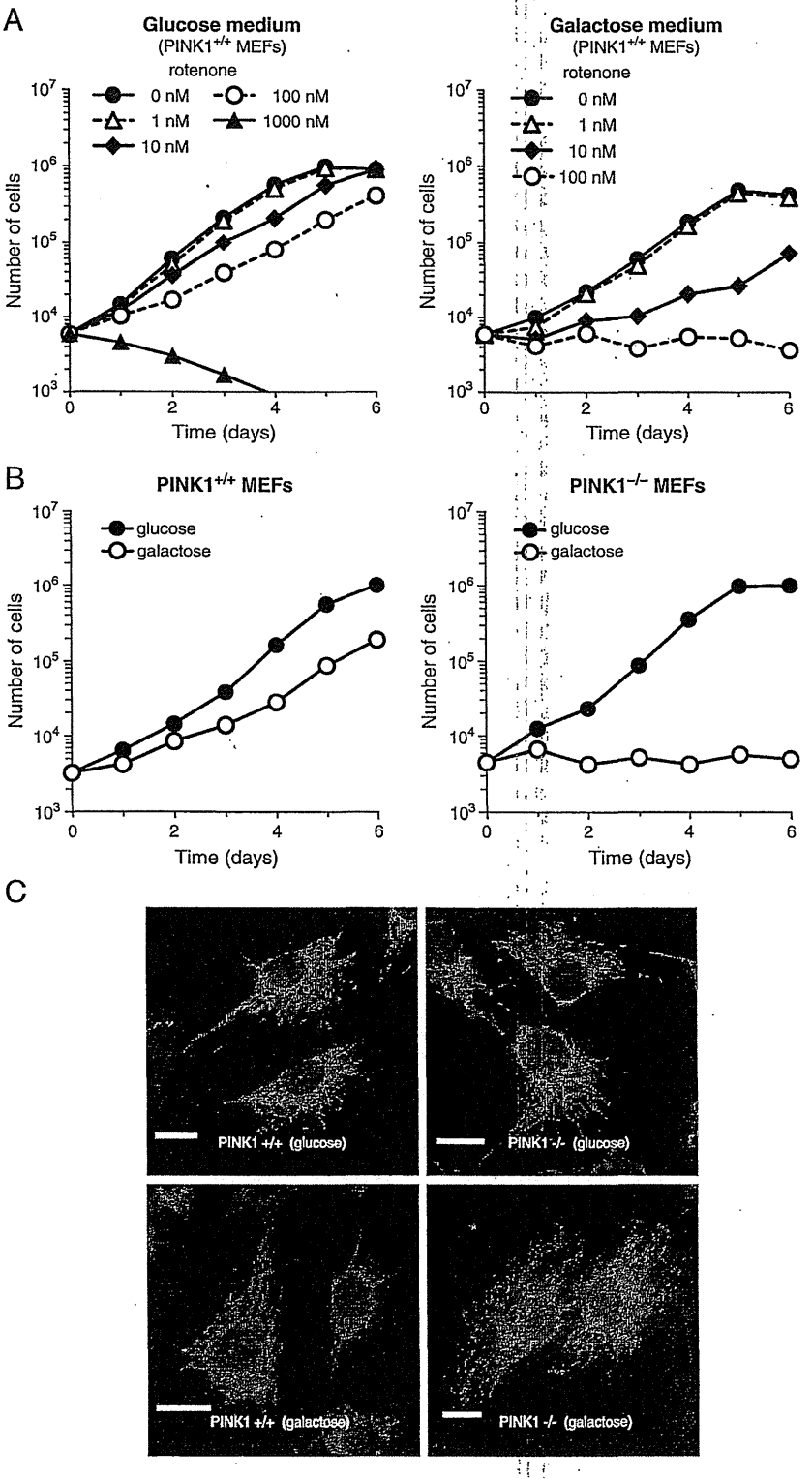

Fig. 1. (A) Growth retardation of PINK1$^{+/+}$ MEFs by mitochondrial complex I inhibitor, rotenone in glucose or galactose medium. Closed circles with solid line, 0 nM rotenone; open triangles with dashed line, 1 nM rotenone; closed diamonds with solid line, 10 nM rotenone; open circles with dashed line, 100 nM rotenone; closed triangles with solid line, 1000 nM rotenone. Cells grown in 12-well plates were trypsinized and live cells were assessed by trypan blue dye exclusion. (B) Growth curves of PINK1$^{+/+}$ and $^{-/-}$ MEFs. Closed symbols (*glucose*), growth curve for cells grown in DMEM containing 4.5 g/l glucose and 1 mM sodium pyruvate; open symbols (*galactose*), growth curve for cells grown in DMEM lacking glucose and containing instead 1.0 g/l galactose and 1 mM sodium pyruvate. Cells grown in 12-well plates were trypsinized and live cells were assessed by trypan blue dye exclusion. (C) Mitochondrial morphology of PINK1$^{+/+}$ and $^{-/-}$ MEFs. After incubating cells with the glucose or galactose medium for 24 hours, cells were fixed and immunostained with anti-Tom20 antibody to visualize mitochondria. Scale bar, 20 μm.

PINK1$^{-/-}$ cells respired significantly slower than the PINK1$^{+/+}$ cells (1.76 ± 0.13 versus 2.95 ± 0.27 ($p<0.01$; $n=5$ independent experiments) and 16.44 ± 1.80 versus 23.50 ± 1.18 nmol O/min/10^6 cells ($p<0.05$; $n=5$ independent experiments), respectively).

The main function of mitochondria is ATP synthesis via oxidative phosphorylation. ATP levels under basal conditions were significantly reduced in PINK1$^{-/-}$ MEFs (Fig. 2B), as reported previously for dissociated PINK1$^{-/-}$ mouse neurons (Gispert et al., 2009) and PINK1

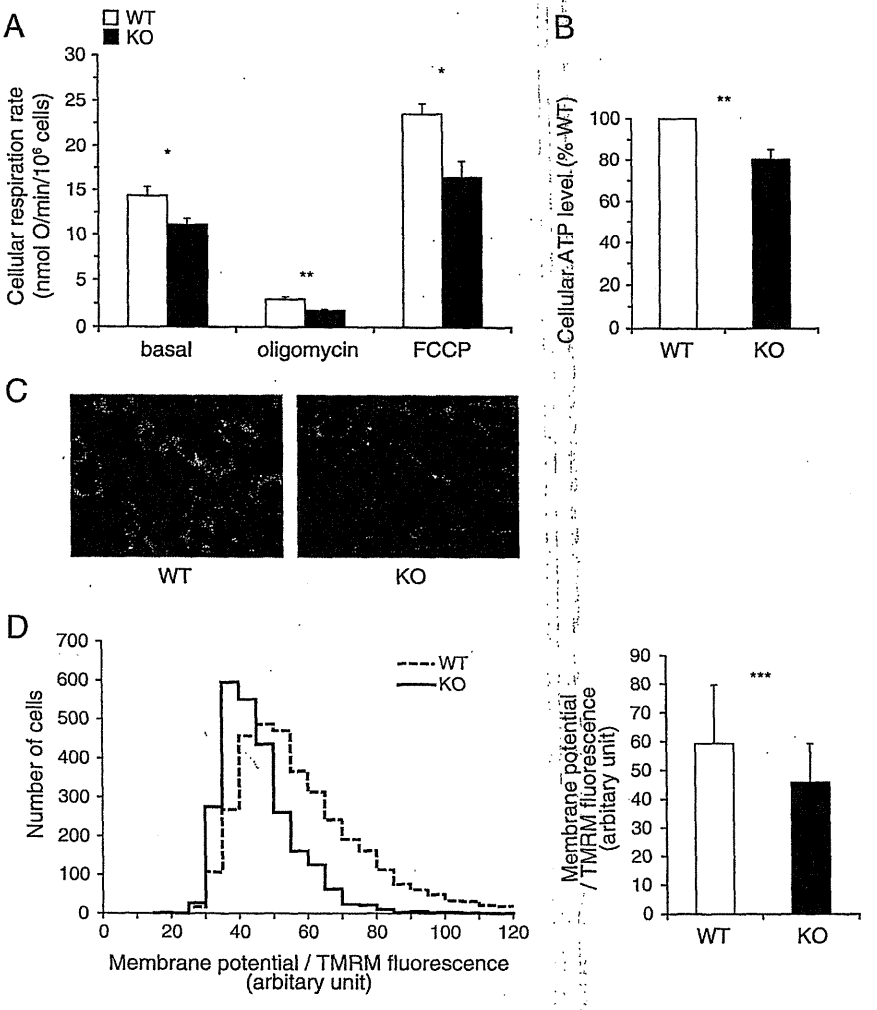

Fig. 2. Mitochondrial functions assessed at the cellular level. Open bars, PINK1$^{+/+}$ MEFs; closed bars, PINK1$^{-/-}$ MEFs. (A) Cell respiration rate of PINK1$^{+/+}$ and $^{-/-}$ MEFs. The oxygen respiration rate was measured at density of 8.0×10^6 cells/ml under each of the following three conditions: basal rate (no additions); State 4 (no ATP synthesis) [after addition of 1 μg/ml oligomycin], uncoupled [after addition of 3 μM FCCP]. After sequential measurements, the endogenous respiration rate was determined by adding 1 μM rotenone + 2 μM myxothiazol. Error bars indicate SEM ($n=5$ independent experiments). (B) Cellular ATP levels. Data were normalized based on cell numbers and expressed as the percentage of the level in PINK1$^{+/+}$ cells. Error bars indicate SEM ($n=4$ independent experiments). (C) Live cell images of PINK1$^{+/+}$ and $^{-/-}$ MEFs with TMRM fluorescence. (D) Mitochondrial membrane potential evaluated by live cell imaging of TMRM fluorescence. *Left panel*, the distribution of TMRM fluorescence from 3537 PIINK1$^{+/+}$ and 2566 PINK1$^{-/-}$ cells from 12 wells per cell type; *right panel*, the average value of TMRM fluorescence per cell. Error bars indicate SD. *$P<0.05$; **$P<0.01$; ***$P<0.001$.

siRNA knock-down PC12 cells (Liu et al., 2009). Mitochondrial membrane potential was also measured by live cell imaging of TMRM fluorescence. Typical images were shown in Fig. 2C. The histogram shows the distribution of TMRM fluorescence from 3537 PINK1$^{+/+}$ cells and 2566 PINK1$^{-/-}$ cells from 12 wells per cell type and the bar graph indicates the mean ± SD of TMRM fluorescence per cell (Fig. 2D). According to the Nernst equation, the ratio of TMRM fluorescence would translate into, on average, 6.88 mV lower mitochondrial membrane potential in the PINK1$^{-/-}$ cells if the plasma membrane potentials were not different between PINK1$^{+/+}$ and $^{-/-}$ cells. Mitochondrial membrane potential decrease was also showed previously in PINK1 knock-down HeLa cells (Exner et al., 2007) and in stable PINK1 knock-down neuroblastoma cell lines (Sandebring et al., 2009).

Assessments of mitochondrial functions using isolated mitochondria

To further analyze mitochondrial functions, we measured the kinetics of oxidative phosphorylation using isolated mitochondria from PINK1$^{+/+}$ and $^{-/-}$ MEFs. Fig. 3 shows the kinetics of the three modules of oxidative phosphorylation using succinate as a respiratory substrate (complex II-linked respiration). Fig. 3A shows the kinetic response of substrate oxidation to its product, $\Delta\psi$. The substrate oxidation kinetic curve for PINK1$^{-/-}$ cells was clearly shifted lower compared with that for PINK1$^{+/+}$ cells, indicating that the loss of PINK1 caused mitochondrial respiratory chain defects. Fig. 3B shows the kinetic response of proton leak to its driving force, $\Delta\psi$, and Fig. 3C shows the kinetic response of the ATP phosphorylating pathway to its driving force, $\Delta\psi$. Both kinetic curves for PINK1$^{+/+}$ and $^{-/-}$ MEFs (open and closed symbols, respectively) were overlapping, implying that there were no significant differences in those modules.

We also independently measured the mitochondrial oxygen consumption rate using pyruvate/malate as a respiratory substrate instead of succinate to check complex I. Modular kinetic analysis using pyruvate/malate is technically difficult for the following reasons: (1) the oxygen consumption rate with pyruvate/malate is much slower than succinate respiration; and (2) there are no competitive inhibitors of complex I-linked respiration, such as malonate for succinate respiration. As shown in Fig. 4A, the respiration rates in State 3 and 4 with pyruvate/malate of isolated mitochondria from PINK1$^{-/-}$ cells (closed symbols) were significantly slower than those of PINK1$^{+/+}$ cells (open symbols), as in the case of succinate respiration (Fig. 4B; data derived from the kinetic curves in Fig. 3).

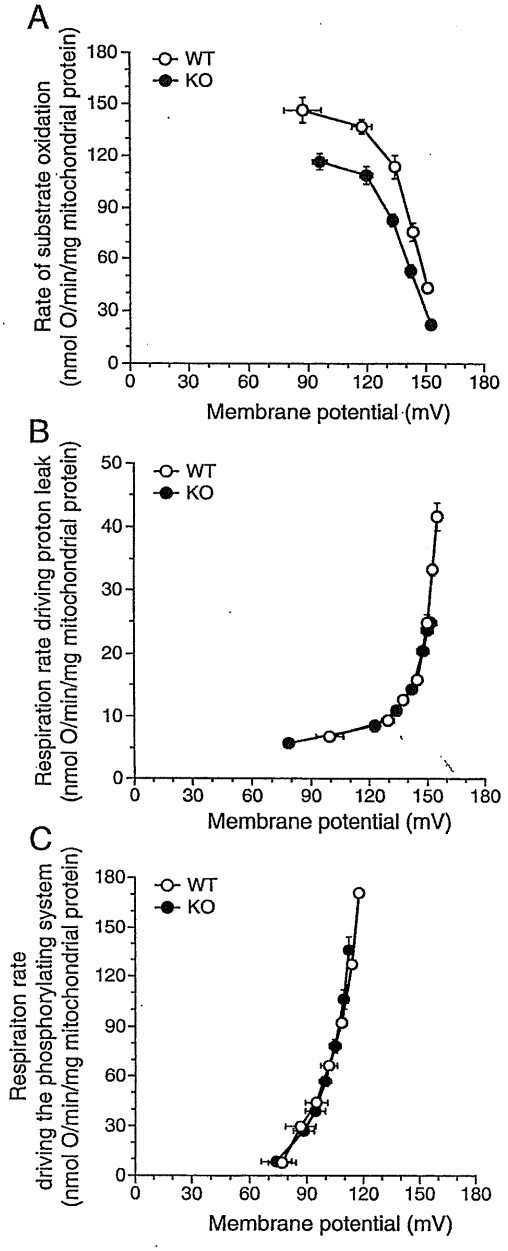

Fig. 3. Modular kinetic analysis of oxidative phosphorylation in mitochondria isolated from PINK1$^{+/+}$ and $^{-/-}$ MEFs. Modular kinetic analysis of the kinetic responses to membrane potential, $\Delta\psi$, of respiration driving (A) substrate oxidation ($\Delta\psi$ titrated with uncoupler, FCCP, starting in State 4), (B) proton leak ($\Delta\psi$ titrated with malonate, starting in State 4) and (C) the phosphorylating system, calculated by subtracting respiration driving proton leak from respiration driving the $\Delta\psi$-consumers ($\Delta\psi$ titrated with malonate starting in State 3; not shown) at each $\Delta\psi$. Open symbols, PINK1$^{+/+}$ MEFs; closed symbols, PINK1$^{-/-}$ MEFs. Error bars indicate SEM ($n=4$ independent mitochondrial preparations).

Mitochondrial ROS production

Mitochondrial ROS production rate was assessed by measurement of the H_2O_2 generation rate. Mechanisms of mitochondrial ROS production were well described elsewhere (Fig. 1 of Lambert et al., 2010). Pyruvate and malate generate NADH, which induced forward electron transport and generate ROS mainly from complex I and III. For pyruvate/malate respiration, the basal H_2O_2 generation rate (measured in the absence of respiratory chain inhibitors) was not different between PINK1$^{+/+}$ and $^{-/-}$ mitochondria (Fig. 4C). The addition of antimycin A and further addition of rotenone, which inhibited forward electron transport at complex III and I, respectively, enhanced H_2O_2 generation. During succinate respiration in the absence of respiratory chain inhibitors, ROS are generated mainly from the quinine binding site of complex I due to reverse electron flow from coenzyme Q to complex I. For succinate respiration, H_2O_2 generation rate in the absence of reparatory chain inhibitors was higher in PINK1$^{+/+}$ mitochondria than in PINK1$^{-/-}$ mitochondria, but the difference was not significant (Fig. 4D). The addition of rotenone, which blocks reverse electron flow from coenzyme Q to complex I, attenuated H_2O_2 generation.

Figs. 4 C and D show a tendency for PINK1$^{+/+}$ mitochondria to generate more ROS than PINK1$^{-/-}$ mitochondria. However, their respiration rates were remarkably different (Figs. 4A and B). Therefore, we calculated the percentage free radical leak, which is the fraction of molecules of O_2 consumed that give rise to H_2O_2 release by mitochondria (free radical leak) during either pyruvate/malate or succinate State 4 respiration (Figs. 4E and F). For pyruvate/malate respiration, mitochondria isolated from PINK1$^{-/-}$ cells had higher proportion of H_2O_2 generation than PINK1$^{+/+}$ mitochondria. During succinate respiration without respiratory inhibitors, PINK1$^{-/-}$ mitochondria had also higher proportion of free radical leak mainly from complex I due to reverse electron flow from coenzyme Q to complex I. Because the differences disappeared with addition of rotenone, which inhibit reverse electron flow, ROS generation enhanced by loss of PINK1 was mostly from complex I.

Discussion

We produced an *in vitro* model of Parkinson's disease, immortalized PINK1$^{-/-}$ MEFs. Previously, impairment of mitochondrial respiration was observed in the brains of PINK1$^{-/-}$ mice (Gautier et al., 2008). PINK1$^{-/-}$ MEFs clearly showed a phenotype of mitochondrial dysfunctions, which is consistent with PD pathogenesis. This phenotype was apparent in a cell growth experiment using medium containing galactose instead of glucose (Fig. 1B). Mitochondrial fragmentation was observed when PINK1$^{-/-}$ MEFs grew in the galactose medium (Fig. 1C), which was consistent with previous reports (Exner et al., 2007; Grünewald et al., 2009). Our results have unveiled that the PINK1$^{-/-}$ MEF line could be a potential PD model, presenting growth retardation due to decreased mitochondrial respiration activity. Thus, the PINK1$^{-/-}$ MEFs are a useful tool for evaluating the role of PINK1 in mitochondrial dysfunction and relevant to PD.

In PINK1$^{-/-}$ MEFs, mitochondrial membrane potential was decreased compared with that in littermate wild-type MEFs (Figs. 2C and D), as reported previously for PINK1 knock-down HeLa cells (Exner et al., 2007) and stable PINK1 knock-down neuroblastoma cell lines (Sandebring et al., 2009). This is a key event during elimination of mitochondria. Mitochondrial fission followed by selective fusion segregates damaged mitochondria, which decreases their membrane potential, and permits their removal by autophagy (Twig et al., 2008). The PINK1–parkin pathway is thought to have a crucial role in this mitochondrial elimination mechanism (Geisler et al., 2010; Kawajiri et al., 2010; Matsuda et al., 2010; Narendra et al., 2008, 2010; Vives-Bauza et al., 2010). To clarify what caused the decrease in mitochondrial membrane potential, we performed a modular kinetic analysis using isolated mitochondria (Fig. 3). This analyzes the kinetics of the whole of oxidative phosphorylation divided into three modules connected by their common substrate or product, mitochondrial membrane potential ($\Delta\psi$). The modules are include one $\Delta\psi$-producer (substrate oxidation) and two $\Delta\psi$-consumers (phosphorylating system and proton leak) (Brand, 1990). To decrease $\Delta\psi$, the $\Delta\psi$-producer should be down-regulated and/or $\Delta\psi$-consumers should be up-regulated. As cellular ATP levels were decreased compared with those in littermate wild-type MEFs (Fig. 2B), it is unlikely that the phosphorylating system is up-regulated. Indeed, the kinetics of the phosphorylation module were not altered (Fig. 3C). The other $\Delta\psi$-consumer, proton leak,

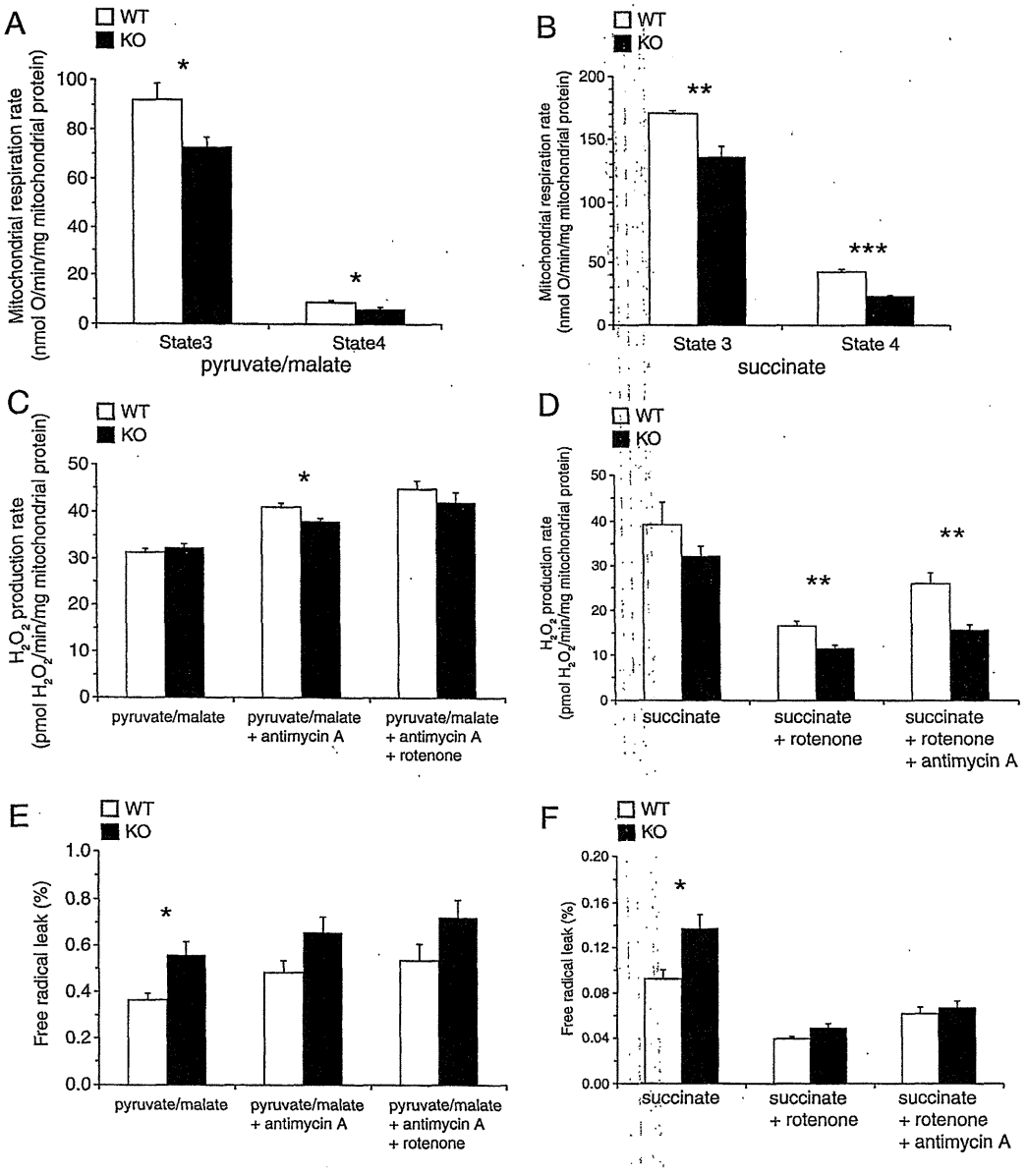

Fig. 4. Oxygen consumption rate and H_2O_2 production rate of mitochondria isolated from PINK1$^{+/+}$ and $^{-/-}$ MEFs. Open bars, PINK1$^{+/+}$ MEFs; closed bars, PINK1$^{-/-}$ MEFs. (A) State 3 and State 4 respiration rate of mitochondria with pyruvate/malate as a respiratory substrate. (B) State 3 and State 4 respiration rate of mitochondria with succinate as a respiratory substrate. Data were derived from the results of modular kinetic analysis (Fig. 3). State 3 respiration rates were the kinetic start points of the $\Delta\psi$-consumers (the sum of the phosphorylating system and proton leak). State 4 respiration rates were average values of the respiration rates at the kinetic start points of substrate oxidation and proton leak. (C, D) Mitochondrial H_2O_2 production rate with pyruvate/malate (C) or succinate (D) as a respiratory substrate. (E, F) Percentage free radical leak (FRL) for State 4 respiration with pyruvate/malate (E) or succinate (F) as a respiratory substrate. Error bars indicate SEM ($n=5$ and 4 independent mitochondrial preparations for pyruvate/malate and succinate respiration, respectively). *$P<0.05$; **$P<0.01$; ***$P<0.001$.

which partially dissipates the membrane potential without ATP synthesis, was also not changed (Fig. 3B). Therefore, the decrease in membrane potential caused by loss of PINK1 is likely to have been caused only by lower activity of the $\Delta\psi$-producer, substrate oxidation (Fig. 3A). This is the first report showing that mitochondrial membrane potential decrease caused by loss of PINK1, which is the key event for the following mitochondrial elimination, was not due to proton leak, but to respiratory chain defects. We used only succinate (a complex II-linked substrate) as a respiratory substrate in the modular kinetic analysis for technical reasons. However, complex I-linked respiration (pyruvate/malate) was also decreased in PINK1$^{-/-}$ MEFs like succinate respiration (Fig. 4A).

The mitochondrial respiration rates in State 4 were decreased in PINK1$^{-/-}$ MEFs, and consequently, the proportions of free radical leak were significantly higher in PINK1$^{-/-}$ MEFs than in PINK1$^{+/+}$ MEFs (Figs. 4E and F). Because the differences disappeared with addition of rotenone (complex I inhibitor, which inhibits reverse electron flow from coenzyme Q to complex I), ROS generation enhanced by loss of PINK1 was mostly from complex I. These results are partially consistent with those in previous reports, suggesting that MPTP and rotenone induce neuronal cell death by inhibiting complex I activity, leading to a PD-like phenotype (Dauer and Przedborski, 2003; Jackson-Lewis and Przedborski, 2007; Trojanowski, 2003).

In this study, we developed an *in vitro* PD model, the PINK1$^{-/-}$ MEF line, and established the experimental conditions for cell growth to detect mitochondrial dysfunction. This is the first report showing that complete ablation of PINK1 causes a decrease in mitochondrial membrane potential, which is not due to proton leak, but to respiratory chain defects.

Supplementary materials related to this article can be found online at doi:10.1016/j.nbd.2010.08.027.

Acknowledgments

This work was supported by a Grant-in-Aid for Scientific Research for Young Scientists (B) from JSPS (T.A. and S.Saiki), a JSPS fellowship (T.A.), Nagao Memorial Fund (S. Saiki) and a Grant from Takeda Scientific Foundation (S. Saiki and T.A.). We thank Dr. Noriyuki Matsuda for assistance to obtain immortalized cells.

References

Abou-Sleiman, P.M., Muqit, M.M., Wood, N.W., 2006. Expanding insights of mitochondrial dysfunction in Parkinson's disease. Nat. Rev. Neurosci. 7, 207–219.
Amo, T., Brand, M.D., 2007. Were inefficient mitochondrial haplogroups selected during migrations of modern humans? A test using modular kinetic analysis of coupling in mitochondria from cybrid cell lines. Biochem. J. 404, 345–351.
Barja, G., Cadenas, S., Rojas, C., Pérez-Campo, R., López-Torres, M., 1994. Low mitochondrial free radical production per unit O_2 consumption can explain the simultaneous presence of high longevity and high aerobic metabolic rate in birds. Free Radic. Res. 21, 317–327.
Brand, M.D., 1990. The proton leak across the mitochondrial inner membrane. Biochim. Biophys. Acta 1018, 128–133.
Brand, M.D., 1995. Measurement of mitochondrial protonmotive force. In: Brown, G.C., Cooper, C.E. (Eds.), Bioenergetics, a practical approach. IRL Press, Oxford, pp. 39–62.
Brand, M.D., 1998. Top-down elasticity analysis and its application to energy metabolism in isolated mitochondria and intact cells. Mol. Cell. Biochem. 184, 13–20.
Brand, M.D., Chien, L.F., Diolez, P., 1994. Experimental discrimination between proton leak and redox slip during mitochondrial electron transport. Biochem. J. 297, 27–29.
Chu, C.T., 2010. Tickled PINK1: mitochondrial homeostasis and autophagy in recessive Parkinsonism. Biochim. Biophys. Acta 1802, 20–28.
Clark, I.E., Dodson, M.W., Jiang, C., Cao, J.H., Huh, J.R., Seol, J.H., Yoo, S.J., Hay, B.A., Guo, M., 2006. *Drosophila pink1* is required for mitochondrial function and interacts genetically with *parkin*. Nature 441, 1162–1166.
Dauer, W., Przedborski, S., 2003. Parkinson's disease: mechanisms and models. Neuron 39, 889–909.
Exner, N., Treske, B., Paquet, D., Holmstrom, K., Schiesling, C., Gispert, S., Carballo-Carbajal, I., Berg, D., Hoepken, H.H., Gasser, T., Krüger, R., Winklhofer, K.F., Vogel, F., Reichert, A.S., Auburger, G., Kahle, P.J., Schmid, B., Haass, C., 2007. Loss-of-function of human PINK1 results in mitochondrial pathology and can be rescued by parkin. J. Neurosci. 27, 12413–12418.
Gandhi, S., Wood-Kaczmar, A., Yao, Z., Plun-Favreau, H., Deas, E., Klupsch, K., Downward, J., Latchman, D.S., Tabrizi, S.J., Wood, N.W., Duchen, M.R., Abramov, A.Y., 2009. PINK1-associated Parkinson's disease is caused by neuronal vulnerability to calcium-induced cell death. Mol. Cell 33, 627–638.
Gautier, C.A., Kitada, T., Shen, J., 2008. Loss of PINK1 causes mitochondrial functional defects and increased sensitivity to oxidative stress. Proc. Natl. Acad. Sci. U. S. A. 105, 11364–11369.
Geisler, S., Holmström, K.M., Skujat, D., Fiesel, F.C., Rothfuss, O.C., Kahle, P.J., Springer, W., 2010. PINK1/Parkin-mediated mitophagy is dependent on VDAC1 and p62/SQSTM1. Nat. Cell Biol. 12, 119–131.
Gispert, S., Ricciardi, F., Kurz, A., Azizov, M., Hoepken, H.H., Becker, D., Voos, W., Leuner, K., Müller, W.E., Kudin, A.P., Kunz, W.S., Zimmermann, A., Roeper, J., Wenzel, D., Jendrach, M., García-Arencíbia, M., Fernández-Ruiz, J., Huber, L., Rohrer, H., Barrera, M., Reichert, A.S., Rüb, U., Chen, A., Nussbaum, R.L., Auburger, G., 2009. Parkinson phenotype in aged PINK1-deficient mice is accompanied by progressive mitochondrial dysfunction in absence of neurodegeneration. PLoS One 4, e5777.
Grünewald, A., Gegg, M.E., Taanman, J.W., King, R.H., Kock, N., Klein, C., Schapira, A.H., 2009. Differential effects of PINK1 nonsense and missense mutations on mitochondrial function and morphology. Exp. Neurol. 219, 266–273.
Haque, M.E., Thomas, K.J., D'Souza, C., Callaghan, S., Kitada, T., Slack, R.S., Fraser, P., Cookson, M.R., Tandon, A., Park, D.S., 2008. Cytoplasmic Pink1 activity protects neurons from dopaminergic neurotoxin MPTP. Proc. Natl. Acad. Sci. U. S. A. 105, 1716–1721.
Hofhaus, G., Johns, D.R., Hurko, O., Attardi, G., Chomyn, A., 1996. Respiration and growth defects in transmitochondrial cell lines carrying the 11778 mutation associated with Leber's hereditary optic neuropathy. J. Biol. Chem. 271, 13155–13161.
Jackson-Lewis, V., Przedborski, S., 2007. Protocol for the MPTP mouse model of Parkinson's disease. Nat. Protoc. 2, 141–151.
Kawajiri, S., Saiki, S., Sato, S., Sato, F., Hatano, T., Eguchi, H., Hattori, N., 2010. PINK1 is recruited to mitochondria with parkin and associates with LC3 in mitophagy. FEBS Lett. 584, 1073–1079.
Kim, Y., Park, J., Kim, S., Song, S., Kwon, S.K., Lee, S.H., Kitada, T., Kim, J.M., Chung, J., 2008. PINK1 controls mitochondrial localization of Parkin through direct phosphorylation. Biochem. Biophys. Res. Commun. 377, 975–980.
King, M.P., Attardi, G., 1989. Human cells lacking mtDNA: repopulation with exogenous mitochondria by complementation. Science 246, 500–503.
Lambert, A.J., Buckingham, J.A., Boysen, H.M., Brand, M.D., 2010. Low complex I content explains the low hydrogen peroxide production rate of heart mitochondria from the long-lived pigeon, Columba livia. Aging Cell 9, 78–91.
Liu, W., Vives-Bauza, C., Acin-Perez, R., Yamamoto, A., Tan, Y., Li, Y., Magrane, J., Stavarache, M.A., Shaffer, S., Chang, S., Kaplitt, M.G., Huang, X.Y., Beal, M.F., Manfredi, G., Li, C., 2009. PINK1 defect causes mitochondrial dysfunction, proteasomal deficit and alpha-synuclein aggregation in cell culture models of Parkinson's disease. PLoS One 4, e4597.
Matsuda, N., Sato, S., Shiba, K., Okatsu, K., Saisho, K., Gautier, C.A., Sou, Y.S., Saiki, S., Kawajiri, S., Sato, F., Kimura, M., Komatsu, M., Hattori, N., Tanaka, K., 2010. PINK1 stabilized by mitochondrial depolarization recruits Parkin to damaged mitochondria and activates latent Parkin for mitophagy. J. Cell Biol. 189, 211–221.
Narendra, D., Tanaka, A., Suen, D.F., Youle, R.J., 2008. Parkin is recruited selectively to impaired mitochondria and promotes their autophagy. J. Cell Biol. 183, 795–803.
Narendra, D.P., Jin, S.M., Tanaka, A., Suen, D.F., Gautier, C.A., Shen, J., Cookson, M.R., Youle, R.J., 2010. PINK1 is selectively stabilized on impaired mitochondria to activate Parkin. PLoS Biol. 8, e1000298.
Park, J., Lee, S.B., Lee, S., Kim, Y., Song, S., Kim, S., Bae, E., Kim, J., Shong, M., Kim, J.M., Chung, J., 2006. Mitochondrial dysfunction in *Drosophila PINK1* mutants is complemented by *parkin*. Nature 441, 1157–1161.
Pridgeon, J.W., Olzmann, J.A., Chin, L.S., Li, L., 2007. PINK1 protects against oxidative stress by phosphorylating mitochondrial chaperone TRAP1. PLoS Biol. 5, e172.
Reitzer, L.J., Wice, B.M., Kennell, D., 1979. Evidence that glutamine, not sugar, is the major energy source for cultured HeLa cells. J. Biol. Chem. 254, 2669–2676.
Reynafarje, B., Costa, L.E., Lehninger, A.L., 1985. O_2 solubility in aqueous media determined by a kinetic method. Anal. Biochem. 145, 406–418.
Sandebring, A., Thomas, K.J., Beilina, A., van der Brug, M., Cleland, M.M., Ahmad, R., Miller, D.W., Zambrano, I., Cowburn, R.F., Behbahani, H., Cedazo-Mínguez, A., Cookson, M.R., 2009. Mitochondrial alterations in PINK1 deficient cells are influenced by calcineurin-dependent dephosphorylation of dynamin-related protein 1. PLoS One 4, e5701.
Trojanowski, J.Q., 2003. Rotenone neurotoxicity: a new window on environmental causes of Parkinson's disease and related brain amyloidoses. Exp. Neurol. 179, 6–8.
Twig, G., Elorza, A., Molina, A.J., Mohamed, H., Wikstrom, J.D., Walzer, G., Stiles, L., Haigh, S.E., Katz, S., Las, G., Alroy, J., Wu, M., Py, B.F., Yuan, J., Deeney, J.T., Corkey, B. E., Shirihai, O.S., 2008. Fission and selective fusion govern mitochondrial segregation and elimination by autophagy. EMBO J. 27, 433–446.
Valente, E.M., Abou-Sleiman, P.M., Caputo, V., Muqit, M.M., Harvey, K., Gispert, S., Ali, Z., Del Turco, D., Bentivoglio, A.R., Healy, D.G., Albanese, A., Nussbaum, R., González-Maldonado, R., Deller, T., Salvi, S., Cortelli, P., Gilks, W.P., Latchman, D.S., Harvey, R.J., Dallapiccola, B., Auburger, G., Wood, N.W., 2004. Hereditary early-onset Parkinson's disease caused by mutations in *PINK1*. Science 304, 1158–1160.
Vives-Bauza, C., Zhou, C., Huang, Y., Cui, M., de Vries, R.L., Kim, J., May, J., Tocilescu, M.A., Liu, W., Ko, H.S., Magrane, J., Moore, D.J., Dawson, V.L., Grailhe, R., Dawson, T.M., Li, C., Tieu, K., Przedborski, S., 2010. PINK1-dependent recruitment of Parkin to mitochondria in mitophagy. Proc. Natl. Acad. Sci. U. S. A. 107, 378–383.
Wood-Kaczmar, A., Gandhi, S., Yao, Z., Abramov, A.Y., Miljan, E.A., Keen, G., Stanyer, L., Hargreaves, I., Klupsch, K., Deas, E., Downward, J., Mansfield, L., Jat, P., Taylor, J., Heales, S., Duchen, M.R., Latchman, D., Tabrizi, S.J., Wood, N.W., 2008. PINK1 is necessary for long term survival and mitochondrial function in human dopaminergic neurons. PLoS One 3, e2455.
Yang, Y., Ouyang, Y., Yang, L., Beal, M.F., McQuibban, A., Vogel, H., Lu, B., 2008. Pink1 regulates mitochondrial dynamics through interaction with the fission/fusion machinery. Proc. Natl. Acad. Sci. U. S. A. 105, 7070–7075.

Phenotype of the 202 Adenine Deletion in the *parkin* Gene: 40 Years of Follow-Up

Sharon Hassin-Baer, MD,[1,2] Nobutaka Hattori, MD, PhD,[3] Oren S. Cohen, MD,[1,2] Magdalena Massarwa, MD,[1] Simon D. Israeli-Korn, MA, MRCP (UK),[1] and Rivka Inzelberg, MD[1,2*]

[1]*The Sagol Neuroscience Center, Department of Neurology, Sheba Medical Center, Tel Hashomer, Israel;* [2]*Sackler Faculty of Medicine, Tel Aviv University, Tel Aviv, Israel;* [3]*Department of Neurology, Juntendo University Medical School, Tokyo, Japan*

ABSTRACT

Background: We describe the four decades follow-up of 14 *parkin* patients belonging to two large eight-generation-long in-bred Muslim-Arab kindreds.

Results: All patients had a single base-pair of adenine deletion at nucleotide 202 of exon 2 (202A) of the *parkin* gene (all homozygous, one heterozygous). Parkinson's disease onset age was 17–68 years. Special features were intractable axial symptoms (low back pain, scoliosis, camptocormia, antecollis), postural tremor, and preserved cognition.

Conclusions: The 202A deletion of the *parkin* gene causes early-onset Parkinson's disease with marked levodopa/STN-DBS–resistant axial features. Postural tremor and preserved cognition, even after 40 years of disease, were also evident. © 2011 *Movement* Disorder Society

Key Words: Parkinson's disease; genetics; Parkin; PARK2; follow-up

Introduction

Mutations in the *parkin* gene (6q25.2-6q27, MIM 602544) are the most common cause of monogenic autosomal recessive Parkinson's disease (PD).[1,2] The phenotype includes early onset of classic PD symptoms, but may vary with respect to additional atypical features.[3–5] Exonic deletions or multiplications and truncating or missense mutations have been described.[1–6] No reports point to ethnic clusters of specific *parkin* mutations. We describe four-decades follow-up of 14 *parkin* patients belonging to two large in-bred Muslim-Arab kindreds.

Methods

PD patients of Arabic-origin with age of disease onset < 50 years were recruited from the Sheba Medical Center Movement Disorders Clinic. The Institutional Review Board approved the use of human subjects for this study. All patients and family members signed informed consent for participating in the study.

Participants were examined by a movement disorders specialist at 2–12 months intervals. Asymptomatic family members were examined once at the time of DNA collection. DNA was extracted from blood leukocytes. All exons of the *parkin* gene were screened for deletions, insertions, or point mutations by direct sequencing of the PCR products, sequenced on both strands as previously described.[4]

Results

Thirteen of 14 PD patients and 15 family members consented to genetic testing. Patient characteristics are summarized in Table 1 (10 men, 4 women; mean age 52 ± 10 years; range 35–73 years).

In all 13 patients, the same *parkin* mutation was found: a single base-pair deletion of adenine at nucleotide 202 of exon 2 (202A), causing an out-frame mutation with an early-stop codon (12 homozygous, 1 heterozygous) and one patient was not genotyped. The mutant *parkin* lacks a part of the Ubl domain and the entire region of the RING box, suggesting loss of activity of E3.

Phenotype and Clinical Course

All patients belong to two large Muslim-Arab in-bred *hamulas* (kindreds). Each *hamula* can trace their ancestry to a few founders about eight generations ago. Family A traced back five generations and divided into three branches shown as Aa, Ab, and Ac Family B traced back eight generations.

Mean age ± SD at PD onset was 31 ± 15 years (range 17–68) and disease duration 21 ± 13 (median 19, range 1–41 years) (Table 1). The first patient (B-VII-22) was seen in our clinic in 1963, aged 27 years. She complained of "bent trunk" and slowing since the age of 23. Her first cousin (B-VII-25) was examined in 1989, aged 19 years due to scolisois and

***Correspondence to:** Dr. Rivka Inzelberg, The Sagol Neuroscience Center, Department of Neurology, Sheba Medical Center, Tel Hashomer, 52621, Israel; inzelber@post.tau.ac.il.

Relevant conflicts of interest/financial disclosures: Nothing to report. Full financial disclosures and author roles may be found in the online version of this article.

Received: 11 July 2010; **Revised:** 31 August 2010; **Accepted:** 3 September 2010
Published online 21 January 2011 in Wiley Online Library (wileyonlinelibrary.com). DOI: 10.1002/mds.23456

Table 1. Demographic characteristics and motor features of Parkinson's disease (PD) patients with the *parkin* 202A deletion

Patient No.	*Parkin* 202A deletion	Gender	Age	Age of onset	PD duration	H&Y stage	Presenting sign	Rest tremor	Rig.	Asym	Brad.	Post. Inst.	Gait dist.	Post. tremor
Aa-II-3	HOM	M	58	17	41	3	Hand tremor	+	+	+	+	+	+	+
Aa-II-8	HOM	M	50	15	35	4	Leg dystonia	+	+	+	+	+	+	+
Aa-II-10	HOM	F	48	47	1	2	Leg tremor		+	+	+		+	
Aa-II-11	HOM	M	47	30	17	3	Leg tremor	+	+	+	+	+	+	+
Ab-IV-14	NG	M	73	68	5	3	Slow gait	+	+	+	+	+	+	
Ab-V-7	HOM	F	47	18	29	3	Hand tremor	+	+	+		+	+	+
Ac-IV-5	HOM	F	35	17	18	4	Hand tremor	+	+	+	+	+	+	+
B-VII-8	HOM	M	62	35	27	4	Leg tremor	+	+	+	+			+
B-VII-10	HOM	M	59	28	31	4	Hand tremor	+	+	+	+	+	+	+
B-VII-13	HOM	M	49	37	12	3	Leg tremor	+	+	+	+			+
B-VII-17	HOM	M	44	30	14	3	Hand tremor	+	+	+	+			+
B-VII-22	HOM	F	63	23	40	3	Camptocormia	+	+	+	+	+	+	+
B-VII-25	HOM	M	39	19	20	3	Hand tremor	+	+	+	+		+	+
Aa-II-6	HET	M	55	49	6	2	Hand tremor		+	+	+			
Mean±SD			52±10	31±15	21±13									

HET, heterozygous; HOM, homozygous; NG, not genotyped; Rig, rigidity; Asym, asymmetry; Brad, bradykinesia; Post Inst, postural instability; Dist, disturbance; Post, postural.

bradykinesia. The diagnosis of juvenile-onset PD was made in both.

The presenting symptom was hand tremor (n = 6), leg tremor (n = 4), foot dystonia (n = 1), camptocormia (n = 1), and gait disturbances (n = 1). Bradykinesia and rigidity were present in all patients and rest tremor in all but one. Eleven had postural hand tremor, three limb dystonia (two at PD onset) and three reported sleep benefit (Table 1).

Atypical motor features included prominent levodopa-resistant axial symptoms (n = 10): recurrent falls at onset (n = 1), gait disturbances at onset (n = 1), scoliosis (n = 1), camptocormia (progressive to fixed 90° trunk flexion, n = 2), antecollis (n = 1), lower back pain (LBP) (n = 8) (Table 2). Camptocormia and antecollis 5 years after onset were observed in a heterozygous carrier with an intermediate PD phenotype (onset 49 years) and very slow disease progression.

Pain was a predominant symptom (painful dystonia = 2, LBP = 8). Two patients manifested autonomic dysfuntion with complaints of constipation (Table 1).

None of the patients developed significant cognitive impairment or dementia during follow-up of up to 40 years (median 19 years). Seven patients had depressive symptoms but none develeoped hallucinosis or psychosis.

Response to Treatment and Progression

Levodopa response was excellent for appendicular signs but only minor for axial signs. All patients devel-

Table 2. Nonmotor/atypical features and therapy-related features of Parkinson's disease (PD) patients with the *parkin* 202A deletion

Patient No.	Psych.	Cognitive decline	Sleep benefit	Autonomic features	Additional axial features	Response to levodopa	Wearing off	Levodopa induced dyskinesia	UPDRS III (on/off)	DBS (Yr after PD onset)
Aa-II-3		–				+	+	+	52	
Aa-II-8	DEP	–	+			+	+	+	20/27	+ (30)
Aa-II-10		–	+	constip	LBP	NA	NA	NA	17/NA	
Aa-II-11		–				+			46	
Ab-IV-14		–		constip		+	+		38/41	
Ab-V-7	DEP	–	+		LBP	+	+	+	14	
Ac-IV-5	DEP	–				+	+	+	48/61	+ (14)
B-VII-8	DEP	–			LBP	+	+	+	16/22	
B-VII-10	DEP	–			LBP	+	+	+	37/64	+ (26)
B-VII-13	DEP	–			LBP	+	+		4/20	
B-VII-17		–			LBP	+	+		20/30	
B-VII-22	DEP	–			Camptocormia, LBP	+	+	+	37/48	
B-VII-25		–			Scoliosis, LBP	+	+	+	16/28	
Aa-II-6		–			Antecollis, Camptocormia	NA	NA	NA	NA	

DEP, depression; constip, constipation; LBP, Lower back pain; NA, not applicable.

oped motor fluctuations. Despite consistently very slow disease progression, three patients developed severe motor fluctuations and underwent deep brain stimulation (STN-DBS) 14, 26, and 30 years after PD onset. Response to STN-DBS was modest with improvement in appendicular symptoms but no change in axial features, particularly postural instability, gait disorders, and LBP.

Genotype and Phenotype of Nonparkinsonian Family Members

Fifteen family members were genotyped. Five had no mutations and 10 were heterozygous, of whom nine were asymptomatic (age range 28–40 years). One family member, (70 year-old female) with postural tremor only (onset 60 years, B-VI-5), showed A-G heterozygosity for the 202A *parkin* deletion. Tremor remained her sole symptom during 10 years of follow-up and was levodopa unresponsive.

Discussion

The marked axial nature is the most striking feature of the *parkin* 202A deletion phenotype. This includes camptocormia, antecollis, scolisosis, and low back pain. Dystonia in PD manifests mainly in the limbs as equinovarus foot, striatal toe, ulnar deviation or hemidystonia and in the mid-line as blepharospasm or oromandibular dystonia.[7] Scoliosis, if considered a form of dystonia, is also seen. Camptocormia is a rare feature of PD and is attributed to dystonia or imbalance in muscle activity.[3,6–8] We postulate that LBP is part of the dystonic phenotype. In our patients, axial symptoms were painful and levodopa/STN-DBS unresponsive.

A second main characterisitic of the 202A *parkin* deletion phenotype was the preserved cognition after several decades since PD onset. Lack of dementia characterizes parkin disease.[9] To our knowledge long term follow-up up to 40 years has not yet been described. It has been suggested that the lack of dementia in parkin disease may be related to the absence of Lewy body pathology.[9] Hayashi et al. reported neuropathologic findings in a Japanese patient with a mutation in the *parkin* gene.[10] Loss of pigmented neurons and gliosis were most pronounced in the medial and ventrolateral regions of the SN pars compacta and in the locus ceruleus. There was no clinical evidence of dementia and no Lewy bodies were identified. Some neurofibrillary tangles and senile plaques were observed in the cerebral cortex. Another study also found diffuse tau pathology but no Lewy bodies.[11] Neuropsychiatric disturbances are reportedly common in carriers for *parkin* or *PINK1* mutations.[12,13] The 202A phenotype commonly included depression.

There is controversy whether heterozygous carriers of *parkin* mutations are symptomatic and whether *parkin* is a susceptibility gene.[14,15] One of our heterozygous patients (onset 49 years) developed a mild phenotype but with antecollis and camptocormia. Another heterozygous family member presented solely with postural tremor (onset 60 years) with no other parkinsonian features during 10 years of follow-up. While homozygous mutations in the *parkin* gene result in early-onset PD, heterozygous mutations in the *parkin* gene are identified in patients with later-onset disease, raising the possibility that heterozygous mutations may have a role beyond that of loss of function and confer an increased susceptibility to the disease.[15]

The risk of developing PD in individuals with mutations in the *parkin* gene is age-dependent and penetrance remains unclear. Our asymptomatic carriers were aged 28–40 years and need to be further followed. A recent study identified mutations in the *parkin* gene in 10% of probands with disease onset before age 50.[16] They estimated the cumulative incidence of PD to age 65 years in relatives of mutation carriers to be 7%, compared to 1.7% in noncarrier relatives, and 1.1% in relatives of controls.

Periquet and coworkers analyzed *parkin* gene inheritance to discriminate between single founder effects and independent recurrent events by the use of intragenic and tightly flanking markers of the *parkin* gene region.[17] By studying a variety of *parkin* mutations in 48 European families they showed that the majority of exon rearrangements result from distinct mutational events, whereas point mutations may have arisen from a limited number of founders suggesting different mechanisms underlying these two groups of mutations. According to this hypothesis, the frequency of exon rearrangements would be expected, in the absence of selection, to increase with the passage of time because of new mutational events, whereas the frequency of point mutations as in our patients would be expected to remain stable, because new mutations would be rare. In this context, the 202A deletion, being a point mutation, could be related to a founder effect which persisted because of high rates of consanguinity in this population.

The fact that all patients in our two kindreds carry the same mutation suggests that it might be common among young-onset PD patients of Arabic descent. Indeed, the 202A deletion has also been observed among Jordanian patients.[17] However, the exact phenotype in this population has not been specified. While PD prevalence above the age of 65 years in Arab villages in Israel is similar to that of Western populations,[18] neither the prevalence of *parkin* mutations nor its impact on PD prevalence in young adults is known. In our studied population of Muslim Arab villages with large in-bred kindreds, carrier frequencies may be high.

Our phenotypic observations might be useful for raising the suspicion and recognition of carriers of the

parkin 202A deletion mutation among young-onset PD patients with Arabic ancestry. Postural tremor, prominent and/or painful axial features, slowness of progression of motor symptoms and preservation cognitive function are strong clues to *parkin* disease.

References

1. Lucking CB, Durr A, Bonifati V, et al. Association between early-onset Parkinson's disease and mutations in the parkin gene. N Engl J Med 2000;342:1560–1567.
2. Kann M, Jacobs H, Mohrmann K, et al. Role of parkin mutations in 111 community-based patients with early-onset parkinsonism. Ann Neurol 2002;51:621–625.
3. Inzelberg R, Hattori N, Nisipeanu P, et al. Camptocormia, axial dystonia, and parkinsonism: phenotypic heterogeneity of a parkin mutation. Neurology 2003;60:1393–1394.
4. Nisipeanu P, Inzelberg R, Abo Mouch S, et al. Parkin gene causing benign autosomal recessive juvenile parkinsonism. Neurology 2001;56:1573–1575.
5. Nisipeanu P, Inzelberg R, Blumen SC, et al. Autosomal-recessive juvenile parkinsonism in a Jewish Yemenite kindred: mutation of Parkin gene. Neurology 1999;53:1602–1604.
6. Kitada T, Asakawa S, Hattori N, et al. Mutations in the parkin gene cause autosomal recessive juvenile parkinsonism. Nature 1998;392:605–608.
7. De Yebenes JC PR, Taberno C. Symptomatic dystonias. In: Watts RL,Koller KW, editors. Movement disorders neurologic principles and practice. New York:McGrawHill;1997. p 455–475.
8. Djaldetti R, Mosberg-Galili R, Sroka H, Merims D, Melamed E. Camptocormia (bent spine) in patients with Parkinson's disease—characterization and possible pathogenesis of an unusual phenomenon. Mov Disord 1999;14:443–447.
9. Inzelberg R, Polyniki A. Are genetic and sporadic Parkinson's disease patients equally susceptible to develop dementia? J Neurol Sci 2010;289:23–26.
10. Hayashi S, Wakabayashi K, Ishikawa A, et al. An autopsy case of autosomal-recessive juvenile parkinsonism with a homozygous exon 4 deletion in the parkin gene. Mov Disord 2000;15:884–888.
11. van de Warrenburg BP, Lammens M, Lucking CB, et al. Clinical and pathologic abnormalities in a family with parkinsonism and parkin gene mutations. Neurology 2001;56:555–557.
12. Ephraty L, Porat O, Israeli-Korn SD, et al. Neuropsychiatric and cognitive features in autosomal-recessive early parkinsonism due to PINK1 mutations. Mov Disord 2007;22:566–569.
13. Kubo S, Hattori N, Mizuno Y. Recessive Parkinson's disease. Mov Disord 2006;21:885–893.
14. Inzelberg R, Hattori N, Mizuno Y. Dopaminergic dysfunction in unrelated, asymptomatic carriers of a single parkin mutation. Neurology 2005;65:1843.
15. Klein C, Lohmann-Hedrich K, Rogaeva E, Schlossmacher MG, Lang AE. Deciphering the role of heterozygous mutations in genes associated with parkinsonism. Lancet Neurol 2007;6:652–662.
16. Wang Y, Clark LN, Louis ED, et al. Risk of Parkinson disease in carriers of parkin mutations: estimation using the kin-cohort method. Arch Neurol 2008;65:467–474.
17. Myhre R, Steinkjer S, Stormyr A, et al. Significance of the parkin and PINK1 gene in Jordanian families with incidences of young-onset and juvenile parkinsonism. BMC Neurol 2008;8:47.
18. Glik A, Masarwa M, Abuful A, et al. Essential tremor might be less frequent than Parkinson's disease in North Israel Arab villages. Mov Disord 2009;24:119–122.

LINGO1 Gene Analysis in Parkinson's Disease Phenotypes

Oswaldo Lorenzo-Betancor, MD,[1,2] Lluís Samaranch, PhD,[1] Elena García-Martín, MD, PhD,[3,4] Sebastián Cervantes, MD,[1,2] José A.G. Agúndez, MD, PhD,[4,5] Félix J. Jiménez-Jiménez, MD, PhD,[6,7] Hortensia Alonso-Navarro, MD, PhD,[8] Antonio Luengo, MD,[9] Francisco Coria, MD, PhD,[10] Elena Lorenzo, BSc,[1] Jaione Irigoyen, RN,[2,11] Pau Pastor, MD, PhD[1,2,11]* The Iberian Parkinson's Disease Genetics Study Group Researchers

[1]Division of Neurosciences, Neurogenetics Laboratory, Center for Applied Medical Research, University of Navarra, Pamplona, Spain; [2]Department of Neurology, Clínica Universidad de Navarra, University of Navarra School of Medicine, Pamplona, Spain; [3]Biochemistry and Molecular Biology, School of Biological Sciences, University of Extremadura, Badajoz, Spain; [4]RIRAAF/RETICS, Redes Temáticas de Investigación Cooperativa en Salud, Instituto de Salud Carlos III, Spain; [5]Department of Pharmacology, Medical School, University of Extremadura, Badajoz, Spain; [6]Department of Medicine-Neurology, Hospital Príncipe de Asturias, Universidad de Alcalá, Madrid, Spain; [7]Department of Neurology, Hospital del Sureste, Arganda del Rey, Madrid, Spain; [8]Department of Neurology, Hospital La Mancha-Centro de Alcázar de San Juan, Ciudad Real, Spain; [9]Service of Neurology, Hospital Universitario La Princesa, Madrid, Spain; [10]Clinic for Nervous System Disorders and Service of Neurology, Hospital Universitario Son Dureta, Palma de Mallorca, Spain; [11]CIBERNED, Centro de Investigación Biomédica en Red de Enfermedades Neurodegenerativas, Instituto de Salud Carlos III, Spain

ABSTRACT

Background: Parkinson's disease (PD) and essential tremor (ET) may share some etiopathogenic factors. A genome-wide association study has shown that *LINGO1* gene variants are associated with increased risk of ET. We hypothesized that *LINGO1* variants could increase susceptibility to PD. Methods: A large series of PD subjects and healthy controls were genotyped for rs9652490 and rs11856808 *LINGO1* single nucleotide polymorphisms (SNPs). Results: We found an increased frequency of the rs11856808$^{T/T}$ genotype in PD compared with controls (odds ratio = 1.46; corrected *P* value = 0.02). A recessive genetic model was the best fit for rs11856808 influence on PD (recessive gene action test: corrected *P* value = 0.01). Stratification analysis showed that rs11856808$^{T/T}$ genotype frequency was higher in the tremor-dominant PD and the classical PD (C-PD) subgroups (recessive gene action test for the C-PD subgroup: corrected *P* value = 0.004). Discussion: Our results indicate that *LINGO1* variants could increase risk of PD, specifically those presenting the non-rigid-akinetic phenotypes, which suggests that *LINGO1* may have a role in the etiology of tremor in PD at least in the Spanish population. ©2011 *Movement* Disorder Society

Key Words: Parkinson's disease; *LINGO1*; essential tremor; genetics; association study

International Journal of Pediatric Otorhinolaryngology 75 (2011) 211–214

Contents lists available at ScienceDirect

International Journal of Pediatric Otorhinolaryngology

journal homepage: www.elsevier.com/locate/ijporl

Prevalence of *GJB2* causing recessive profound non-syndromic deafness in Japanese children

Chieri Hayashi [a,*], Manabu Funayama [b], Yuanzhe Li [c], Kazusaku Kamiya [a], Atsushi Kawano [d], Mamoru Suzuki [d], Nobutaka Hattori [b,c], Katsuhisa Ikeda [a]

[a] Department of Otorhinolaryngology, Juntendo University School of Medicine, 2-1-1 Hongo, Bunkyo-ku, Tokyo 113-8421, Japan
[b] Research Institute for Diseases of Old Age, Juntendo University School of Medicine, Japan
[c] Department of Neurology, Juntendo University School of Medicine, Japan
[d] Department of Otorhinolaryngology, Tokyo Medical University School of Medicine, Tokyo, Japan

ARTICLE INFO

Article history:
Received 14 June 2010
Received in revised form 18 October 2010
Accepted 2 November 2010
Available online 26 November 2010

Keywords:
Congenital deafness
Cochlear implantation
Japanese children
p.P225L
Connexin 26
GJB2

ABSTRACT

Objective: *GJB2* (gap junction protein, beta 2, 26 kDa: connexin 26) is a gap junction protein gene that has been implicated in many cases of autosomal recessive non-syndromic deafness. Point and deletion mutations in *GJB2* are the most frequent cause of non-syndromic deafness across racial groups. To clarify the relation between profound non-syndromic deafness and *GJB2* mutation in Japanese children, we performed genetic testing for *GJB2*.
Methods: We conducted mutation screening employing PCR and direct sequencing for *GJB2* in 126 children who had undergone cochlear implantation with congenital deafness.
Results: We detected 10 mutations, including two unreported mutations (p.R32S and p.P225L) in *GJB2*. We identified the highest-frequency mutation (c.235delC: 44.8%) and other nonsense or truncating mutations, as in previous studies. However, in our research, p.R143W, which is one of the missense mutations, may also show an important correlation with severe deafness.
Conclusion: Our results suggest that the frequencies of mutations in *GJB2* and *GJB6* deletions differ among cohorts. Thus, our report is an important study of *GJB2* in Japanese children with profound non-syndromic deafness.

1. Introduction

People with any degree of sensory impairment may encounter problems such as discrimination within the education system or when looking for work, and a reduced life expectancy. Sensorineural hearing loss (SNHL) is the most common sensory impairment in developed societies [1,2], where one child in 1000 presents at birth with severe or profound deafness [3].

Recent advances in human genetics have indicated that more than half of congenital SNHL cases involve a genetic factor [4]. In 75–80% of genetic cases, SNHL is the result of autosomal recessive inheritance, and both parents have normal hearing [5]. Mutations of *GJB2* are the most frequent cause of autosomal recessive non-syndromic deafness. Indeed, previous studies have shown that *GJB2* mutations account for up to 50% of non-syndromic deafness cases [6]. Hearing-impaired subjects with biallelic *GJB2* mutations range widely but most commonly follow a severe to profound and non-progressive pattern [7–9]. About 100 different *GJB2* mutations have been reported globally [the Connexin-Deafness homepage: http://davinci.crg.es/deafness/], and these mutations show a relatively high local dependence (founder effect). A high prevalence of c.35delG has been found among Caucasians; c.235delC among Eastern Asians, including Japanese [10–13]; c.167delT among Ashkenazi Jews [14]; p.R143W among certain Africans [15]; and p.W24X among Indians [16,17] and European Gypsies [18–20]. Some recent reports have indicated a genotype-phenotype correlation: children with two truncating mutations, such as c.35delG or c.235delC, are profoundly deaf, while children with a truncating and missense mutation, or two missense mutations, show better hearing [9,21,22]. Since improved speech performance after cochlear implantation in early childhood is usually observed in hearing-impaired subjects with *GJB2* mutations [23], the genetic testing of newborn babies will provide useful prognostic information when selecting appropriate treatment for such children.

In the present study, to clarify the frequency and genotype-phenotype correlation of *GJB2* mutations in children with profound non-syndromic deafness, we performed genetic testing for *GJB2* mutations involving 119 Japanese children who had undergone cochlear implantation with congenital deafness.

* Corresponding author. Tel.: +81 3 5802 1229; fax: +81 3 5840 7103.
E-mail address: chieri-h@juntendo.ac.jp (C. Hayashi).

0165-5876/$ – see front matter © 2010 Elsevier Ireland Ltd. All rights reserved.
doi:10.1016/j.ijporl.2010.11.001

2. Materials and methods

2.1. Subjects

We enrolled 119 Japanese children, who were unrelated to each other, with non-syndromic deafness for genetic analysis. Of these, 107 were sporadic cases (with only one affected individual in the family); the remaining 12 patients were autosomal recessive cases (with normal hearing parents and at least two affected children). The study sample consisted of 70 males (58.8%) and 49 females (41.2%). All of their hearing impairment levels were severe (71–95 dB) to profound (>95 dB); impairments were detected between 0 and 3 years old. All children had undergone cochlear implantation at Tokyo Medical University School of Medicine.

All cases underwent otoscopic examination and audiometric testing. Subjective tests of hearing acuity were assessed based on the auditory brain-stem response (ABR) and auditory steady-state response (ASSR) in infants and children. Behavioral observation audiometry (BOA) was used as a subsidiary measure to ABR and ASSR. A detailed history was taken to exclude other possible causes of deafness (such as neonatal complications, bacterial meningitis or other infections, use of ototoxic medication, or head trauma). Extended pedigrees were elicited from each family to exclude interfamilial relations. Temporal bone computed tomography was used in children to exclude any anomalies. The control group was carefully chosen to determine the carrier frequency, and consisted of 150 unrelated individuals with normal hearing.

Informed consent was obtained from the parents or guardians when necessary, and these were approved by the Ethical Committees of Juntendo University School of Medicine.

2.2. Genetic analysis

All samples from the children and normal controls were extracted from peripheral blood using the QIAamp DNA Blood Mini Kit (QIAGEN, Germantown, MD, USA). The coding region of *GJB2* was amplified from DNA samples by the polymerase chain reaction (PCR) using the primers *GJB2*-F 5′-GTGTGCATTCGTCTTTTCCAG-3′ and *GJB2*-R 5′-GCGACTGAGCCTTGACA-3′. PCR products were sequenced using the PCR primers and sequence primers *GJB2*-A 5′-CCACGCCAGCGCTCCTAGTG-3′ and *GJB2*-B 5′-GAAGATGCTGCT GCTTGTGTAGG-3′. The sequencing reaction products were electrophoresed on an ABI Prism 310 Analyzer (Applied Biosystems). When no mutation or a single heterozygous mutation in *GJB2* was confirmed, we performed the multiplex PCR assay and direct sequencing for the coding region of *GJB6*. Multiplex PCR was carried out according to the method of Del Castillo et al. [24] to confirm the presence of the del(*GJB6*-D13S1830) and del(*GJB6*-D13S1854) deletions in *GJB6*.

Samples with no mutation or a single heterozygous mutation in *GJB2* and *GJB6* were analyzed for the gene dosage using real-time quantitative PCR (qPCR) to detect exon rearrangements in *GJB2* and *GJB6*. qPCR was performed with TaqMan Gene Expression Assays (Hs00269615_s1 for *GJB2*, and Hs00272726_s1 for *GJB6*, Applied Biosystems) and the 7500 Fast Real-Time PCR System (Applied Biosystems).

We obtained blood samples from the family which had one of two unreported mutations, pP225L, and the unreported one was confirmed as follows. The samples were subjected to mutation screening by PCR and direct sequencing for *GJB2*. The PCR product was subcloned into pCR 2.1 vecto-TOPO by TOPO TA cloning (Invitrogen, Carlsbad, CA, USA), and independent subclones were sequenced employing M13forward (5_-TTGTAAAACGACGGCCAG) and reverse (5_-ACACAGGAAACAGCTATG) primers. The sequence data using in this study have been submitted to the GenBank databases under accession numbers X65361, AB098335, NM_000816, and NM_001037.

2.3. Statistical analysis

A *Z*-test was used to calculate the difference in the allele frequency. In all statistical analyses, *P*-values of 0.01 or less were considered significant.

3. Results

3.1. Mutation screening of GJB2

GJB2 mutations were found in 45 of the 119 affected individuals, and, of these, 35 patients were homozygous or compound heterozygous (29.4%). *GJB2*-related deafness patients, who had two *GJB2* mutant alleles, were found in 7 of 12 familial cases (58.3%), and there were 28 of 107 sporadic cases (26.2%). Eight mutations, including two unreported ones (p.R32S and p.P225L), were identified in these patients (Table 1). Three mutations were truncating mutations [one was a nonsense mutation (p.Y136X), and two were frameshifts (c.235delC and c.176-191del)]. The remaining five were missense mutations (p.R143W, p.G45E, p.T86R, p.R32S, and p.P225L). Among these mutations, c.235delC was the most frequent. The c.235delC mutation accounted for 52.9% (37 of 70) of the *GJB2*-mutated alleles (Table 1).

We identified 10 subjects who had three or more mutations. All of them had p.G45E and p.Y136X, including one homozygous child. TA cloning and sequencing of subcloned PCR products revealed that all subjects had both mutations in the same allele (data not shown). G45E accompanied with Y136X has been reported as a pathogenic mutation in previous reports, especially in Japanese patients [11,25], although it remains unclear which mutation is more related to the pathogenicity.

We compared the allele frequency for each mutation with that in Ohtsuka's study [25] (Fig. 1). The frequency of c. 235delC and three mutations (p.R143W, p.G45E/Y136X, and c.176-191del) in this study were significantly different from that in Ohtsuka's study ($P < 0.01$). While the p.V37I mutation was reported to be the second most frequent autosomal recessive deafness allele in Asian countries [11,12], the present subjects did not follow this pattern.

In one subject, we identified a missense mutation, p.P225L, which has not previously been reported (Fig. 2). The sister and father of the proband had this mutation, while they showed a normal hearing function. The mother, with a normal hearing function, showed no mutation at this site, while she revealed only heterozygous p.G45E/Y136X mutation as a known pathogenic mutation of *GJB2*. The sequencing results of TA cloning further confirmed the existence of the pP225L nonsense mutation in this patient. We also identified another unreported mutation, p.R32S, in another subject. The patient had p.R32S/p.G45E/Y136X mutations. The amino acid positions of two unreported mutations

Table 1
Mutations identified in the Cx26 gene, *GJB2* (NG_008358.1), in child cases of congenital deafness.

Nucleotide change	Amino acid change	Allele (%)
c.235delC	p.Leu79CysfsX3	37 (52.9)
c.427C>T	p.Arg143Trp(p.R143W)	15 (21.4)
c.134G>A/c.408C>A	p.Gly45Glu/p.Tyr136X(p.G45E/Y136X)	10 (14.3)
c.176_191del	p.Gly59AlafsX18	4 (5.7)
c.257C>G	p.Thr86Arg(p.T86R)	2 (2.9)
c.94C>A	p.Arg32Ser[a](p.R32S)	1 (1.4)
c.674C>T	p.Pro225Leu[a](p.P225L)	1 (1.4)
Total mutations		70 (100)

[a] Novel mutations detected in this study.

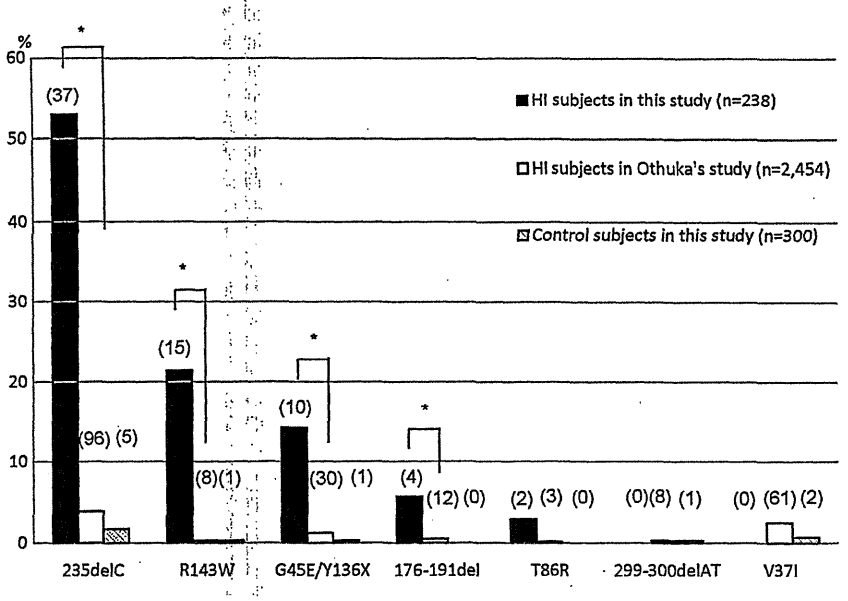

Fig. 1. Allele frequency for each mutation in three groups. A Z-test was used to assess the difference in frequency. Note the *P*-value of <0.01 between the two deafness groups for c.235delC, p.R143W, p.G45E/Y136X, and c.176-191del. *$P < 0.01$.

(p.R32S and p.P225L) are highly conserved among various species, and we did not detect any of these mutations in 300 chromosomes in normal Japanese controls.

4. Discussion

In this study, *GJB2*-related deafness patients accounted for 29.4% of non-syndromic deafness cases. This frequency was less than in a previous report, which pointed to a frequency of around 50% [6]. Familial cases were twice as prevalent as sporadic cases. In most of the previously reported studies, the prevalence of *GJB2* mutations was significantly higher in familial non-syndromic deafness than in sporadic cases [7,26,27]. The frequent mutations of *GJB2* (c.235delC, p.R143W, p. G45E/Y136X, and c.176-191del) in this study were partly different from previous reports [25]. It is assumed that all of our subjects had severe to profound deafness, as they had received cochlear implants, whereas Ohtsuka's subjects had mild to profound deafness and included heterozygous mutations. A few studies have confirmed that some genotypes are correlated with clinical phenotypes in *GJB2*-related deafness. Further, truncating mutations are associated with a greater degree of deafness than non-truncating mutations [9,21,22]. For this reason, three of these cases might be truncating mutations. In contrast, p.R143W mutation was previously implicated in an extraordinarily high prevalence of profound deafness in Ghana [15,28] and Caucasians [9]. This missense mutation may also show an important correlation with severe deafness in Japan. On the other hand, an effect of geography on the allele frequency may have been present, because most of our subjects were from a different area compared to a previous report [25].

The relation between p.V37I mutation of *GJB2* and SNHL is controversial. While some reports suggest that this mutation is

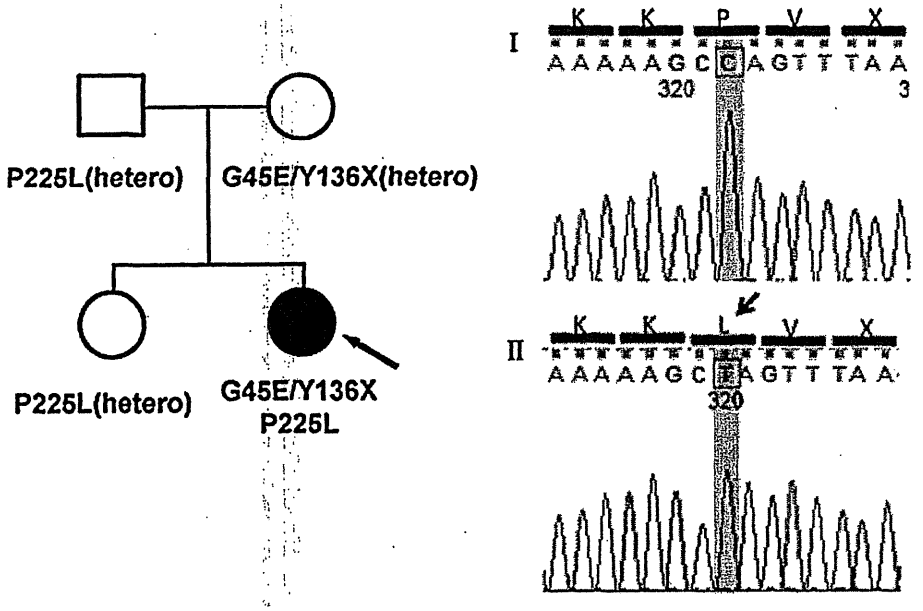

Fig. 2. (A) The pedigree and PCR direct sequencing results for the family; the arrow indicates the proband. (B) The sequencing results on TA cloning. Genomic PCR products were subcloned into a plasmid vector and sequenced separately (see Section 2). The sequences from independent clones are shown in the above two examples. I shows wild-type sequence, whereas II shows mutated sequence in which the proline residue is changed to leucine. Three of 8 subclones showed a missense mutation similar to that in II.

more common among individuals of Asian ancestry [11,12,29], others suggest that homozygous p.V37I is associated with slight/mild hearing loss [22,30,31]. In this study, no cases of homozygous p.V37I were observed. These findings support that this mutation is associated with mild hearing loss, because all of our subjects showed severe deafness.

The two unreported *GJB2* mutations, p.R32S and p.P225L, were not detected in normal hearing controls. These appeared in amino acid residues that were highly conserved. Additionally, three types of mutation were seen in arginine as the thirty-second amino acid, such as p.R32C, p.R32L, and p.R32H. Therefore, R32 is thought to be a mutation "hot spot." Thus, it is likely that these are pathological mutations, rather than rare or functionally neutral polymorphic changes. On the other hand, the mutation site of p.P225 located at the C-terminus of Connexin26 has not previously been reported. As the C-terminus region of connexins is thought to be an important region for intracellular molecular signaling and interaction with scaffolding proteins and the cytoskeleton [32–34], p.P225L mutation found in this study may affect important intracellular molecular networks to maintain the normal function of the cochlear gap junction.

5. Conclusion

In conclusion, this study identified significant genotypic features of Japanese children with profound non-syndromic deafness. Further research is required covering a broader range of genes in the subjects in this study with either single heterozygous or no mutation, in order to better understand the epidemiology of deafness in Japan.

Acknowledgements

We thank all the subjects who participated in the present study. We also thank Ms. Naoko Tamura and Ms. Tomoko Kataoka (Tokyo Medical University School of Medicine), for recruiting families with non-syndromic deafness, and Ms. Junko Onoda (Juntendo University School of Medicine) for assisting in our experiments.

References

[1] A.C. Davis, The prevalence of deafness and reported hearing disability among adults in Great Britain, Int. J. Epidemiol. 18 (1989) 911–917.
[2] D.H. Wilson, P.G. Walsh, L. Sanchez, The epidemiology of deafness in an Australian adult population, Int. J. Epidemiol. 28 (1999) 247–252.
[3] N.E. Morton, Genetic epidemiology of deafness, Ann. N. Y. Acad. Sci. 630 (1991) 1631.
[4] M.L. Marazita, L.M. Ploughman, B. Rawlings, E. Remington, K.S. Arnos, W.E. Nance, Genetic epidemiological studies of early-onset deafness in the U.S. school-age population, Am. J. Med. Genet. 46 (1993) 486–491.
[5] V. Kalatzis, C. Petit, The fundamental and medical impacts of recent progress in research on hereditary hearing loss, Hum. Mol. Genet. 7 (1998) 1589–1597.
[6] A. Kenneson, K. Van Naarden Braun, C. Boyle, GJB2 (connexin 26) variants and nonsyndromic sensorineural hearing loss: a HuGE review, Genet. Med. 4 (2002) 258–274.
[7] F. Denoyelle, S. Marlin, D. Weil, L. Moatti, P. Chauvin, E.N. Garabedian, et al., Clinical features of the prevalent form of childhood deafness, DFNB1, due to a connexin-26 gene defect: Implications for genetic counselling, Lancet 353 (1999) 1298–1303.
[8] A. Murgia, E. Orzan, R. Polli, M. Martella, C. Vinanzi, E. Leonardi, et al., Cx26 deafness: mutation analysis and clinical variability, J. Med. Genet. 36 (1999) 829–832.
[9] R.L. Snoeckx, P.L. Huygen, D. Feldmann, S. Marlin, F. Denoyelle, J. Waligora, et al., *GJB2* mutations and degree of hearing loss: a multicenter study, Am. J. Hum. Genet. 77 (2005) 945–957.
[10] Y. Fuse, K. Doi, T. Hasegawa, A. Sugii, H. Hibino, T. Kubo, Three novel connexin26 gene mutations in autosomal recessive non-syndromic deafnesss, Neuro Report 10 (1999) 1853–1857.
[11] S. Abe, S. Usami, H. Shinkawa, P.M. Kelley, W.J. Kimberling, Prevalent connexin 26 gene (*GJB2*) mutations in Japanese, J. Med. Genet. 37 (2000) 41–43.
[12] T. Kudo, K. Ikeda, S. Kure, Y. Matsubara, T. Oshima, K. Watanabe, et al., Novel mutations in the connexin 26 gene (*GJB2*) responsible for childhood deafness in the Japanese population, Am. J. Med. Genet. 90 (2000) 141–145.
[13] H.J. Park, S.H. Hahn, Y.M. Chun, K. Park, H.N. Kim, Connexin 26 mutations associated with nonsyndromic hearing loss, Laryngoscope 110 (2000) 1535–1538.
[14] P. Gasparini, R. Rabionet, G. Barbujani, S. Melchionda, M. Petersen, K. Brondum-Nielsen, et al., High carrier frequency of the 35delG deafness mutation in European populations, Genetic Analysis Consortium of GJB2 35delG, Eur. J. Hum. Genet. 8 (2000) 19–23.
[15] G.W. Brobby, B. Muller-Myhsok, R.D. Horstmann, Connexin 26 R143W mutation associated with recessive nonsyndromic sensorineural deafness in Africa, N. Engl. J. Med. 338 (1998) 548–550.
[16] M. Maheshwari, R. Vijaya, M. Ghosh, S. Shastri, M. Kabra, P.S. Menon, Screening of families with autosomal recessive non-syndromic hearing impairment (ARNSHI) for mutations in GJB2 gene: Indian scenario, Am. J. Med. Genet. A 120A (2003) 180–184.
[17] M. RamShankar, S. Girirajan, O. Dagan, H.M. Ravi Shankar, R. Jalvi, R. Rangasayee, et al., Contribution of connexin26 (GJB2) mutations and founder effect to non-syndromic hearing loss in India, J. Med. Genet. 40 (2003) e68.
[18] G. Minárik, V. Ferák, E. Feráková, A. Ficek, H. Poláková, L. Kádasi, High frequency of GJB2 mutation W24X among Slovak Romany (Gypsy) patients with non-syndromic hearing loss (NSHL), Gen. Physiol. Biophys. 22 (2003) 549–556.
[19] P. Seeman, M. Malíková, D. Rasková, O. Bendová, D. Groh, M. Kubálková, et al., Spectrum and frequencies of mutations in the GJB2 (Cx26) gene among 156 Czech patients with pre-lingual deafness, Clin. Genet. 66 (2004) 152–157.
[20] A. Alvarez, I. del Castillo, M. Villamar, L.A. Aguirre, A. González-Neira, A. López-Nevot, et al., High prevalence of the W24X mutation in the gene encoding connexin-26 (GJB2) in Spanish Romani (gypsies) with autosomal recessive non-syndromic hearing loss, Am. J. Med. Genet. A 137A (2005) 255–258.
[21] K. Cryns, E. Orzan, A. Murgia, P.L. Huygen, F. Moreno, I. del Castillo, et al., A genotype-phenotype correlation for *GJB2* (connexin 26) deafness, J. Med. Genet. 41 (2004) 147–154.
[22] T. Oguchi, A. Ohtsuka, S. Hashimoto, A. Oshima, S. Abe, Y. Kobayashi, et al., Clinical features of patients with *GJB2* (connexin 26) mutations: Severity of hearing loss is correlated with genotypes and protein expression patterns, J. Hum. Genet. 50 (2005) 76–83.
[23] K. Fukushima, K. Sugata, N. Kasai, S. Fukuda, R. Nagayasu, N. Toida, et al., Better speech performance in cochlear implant patients with GJB2-related deafness, Int. J. Pediatr. Otorhinolaryngol. 62 (2002) 151–157.
[24] F.J. Del Castillo, M. Rodriguez-Ballesteros, A. Alvarez, T. Hutchin, E. Leonardi, C.A. de Oliveira, et al., A novel deletion involving the connexin-30 gene, del(*GJB6*-d13s1854), found in trans with mutations in the *GJB2* gene (connexin-26) in subjects with DFNB1 non-syndromic deafnesss, J. Med. Genet. 42 (2005) 588–594.
[25] A. Ohtsuka, I. Yuge, S. Kimura, A. Namba, S. Abe, L. Van Laer, et al., *GJB2* deafness gene shows a specific spectrum of mutations in Japan, including a frequent founder mutation, Hum. Genet. 112 (2003) 329–333.
[26] J. Loffler, D. Nekahm, A. Hirst-Stadlmann, B. Gunther, H.J. Menzel, G. Utermann, et al., Sensorineural hearing loss and the incidence of Cx26 mutations in Austria, Eur. J. Hum. Genet. 9 (2001) 226–230.
[27] A. Pampanos, J. Economides, V. Iliadou, P. Neou, P. Leotsakos, N. Voyiatzis, et al., Prevalence of *GJB2* mutations in prelingual deafness in the Greek population, Int. J. Pediatr. Otorhinolaryngol. 65 (2002) 101–108.
[28] C. Hamelmann, G.K. Amedofu, K. Albrecht, B. Muntau, A. Gelhaus, G.W. Brobby, et al., Pattern of connexin 26 (*GJB2*) mutations causing sensorineural deafness in Ghana, Hum. Mutat. 18 (2001) 84–85.
[29] WangYC, C.Y. Kung, M.C. Su, C.C. Su, H.M. Hsu, C.C. Tsai, et al., Mutations of Cx26 gene (*GJB2*) for prelingual deafness in Taiwan, Eur. J. Hum. Genet. 10 (2002) 495–498.
[30] C. Huculak, H. Bruyere, T.N. Nelson, F.K. Kozak, S. Langlois, V37I connexin 26 allele in patients with sensorineural hearing loss: Evidence of its pathogenicity, Am. J. Med. Genet. A 140 (2006) 2394–2400.
[31] H.H. Dahl, K. Saunders, T.M. Kelly, A.H. Osborn, S. Wilcox, B. Cone-Wesson, et al., Prevalence and nature of connexin 26 mutations in children with non-syndromic deafnesss, Med. J. Aust. 175 (2001) 191–194.
[32] L.A. Elias, D.D. Wang, A.R. Kriegstein, Gap junction adhesion is necessary for radial migration in the neocortex, Nature 448 (2007) 901–907.
[33] P.E. Martin, G. Blundell, S. Ahmad, R.J. Errington, W.H. Evans, Multiple pathways in the trafficking and assembly of connexin 26, 32 and 43 into gap junction intercellular communication channels, J. Cell Sci. 114 (2001) 3845–3855.
[34] K.A. Schalper, N. Palacios-Prado, M.A. Retamal, K.F. Shoji, A.D. Martínez, J.C. Sáez, Connexin hemichannel composition determines the FGF-1-induced membrane permeability and free $[Ca^{2+}]i$ responses, Mol. Biol. Cell 19 (2008) 3501–3513.

Review

Cell PRESS

Genetic mutations and functions of PINK1

Sumihiro Kawajiri, Shinji Saiki, Shigeto Sato and Nobutaka Hattori

Department of Neurology, Juntendo University School of Medicine, 2-1-1 Hongo, Bunkyo-ku, Tokyo, 113-8421, Japan

Parkinson's disease (PD) is the second most common neurodegenerative disease. Mutations in *PINK1* (*PARK6*) are the second most frequent cause of autosomal recessive, young-onset PD, after *parkin* (*PARK2*). PINK1 (a kinase with an N-terminal mitochondrial targeting sequence) provides protection against mitochondrial dysfunction and regulates mitochondrial morphology via fission/fusion machinery. PINK1 also acts upstream of parkin (a cytosolic E3 ubiquitin ligase) in a common pathway. Recent studies have described PINK1/parkin function in the maintenance of mitochondrial quality via autophagy (mitophagy). PINK1/parkin-mediated mitophagy provides new insights into the etiology of PD and could be a suitable target for new treatment of PD. In this review, we discuss the molecular genetics and functions of PINK1, which could be key factors in novel rational therapy for sporadic PD as well as *PINK1*-linked PD.

Parkinson's disease (PD)

PD is the second most common neurodegenerative disease worldwide after Alzheimer's disease. The prevalence of PD increases with age, and is estimated to be ~1% in those aged > 65 years [1]. The major clinical features are: (i) motor symptoms (called 'parkinsonism'), which include resting tremor, rigidity, bradykinesia (slowness in executing movement) and postural instability; and (ii) non-motor symptoms (e.g. cognitive dysfunction, autonomic nervous system dysfunction, sleep disorders). Pathological features include pronounced loss of dopaminergic neurons in the substantia nigra pars compacta and eosinophilic cytoplasmic inclusion containing α-synuclein aggregates (known as Lewy bodies) in the remaining dopaminergic neurons. No treatment is available to suppress the progression of cell death, and the goal of current therapies is only to alleviate symptoms.

The pathogenesis of PD remains unclear, although mitochondrial dysfunction due to oxidative stress has been proposed to play a major part [2]. Most cases of PD are sporadic, but ~5–10% of PD cases are hereditary. Several genes (e.g. *α-synuclein, parkin, PTEN-induced putative kinase 1* (*PINK1*), *DJ-1, leucine rich repeat kinase 2* (*LRRK2*)) have been identified as causative genes for familial Parkinson's disease (FPD) [3]. *PINK1*-linked PD (*PARK6*-linked PD) is the second most common autosomal recessive young-onset PD, after *parkin*-linked PD (*PARK2*-linked PD). Initial studies suggested that PINK1 provided protection against mitochondrial dysfunction [4–6]. However, the exact function of PINK1 remains unclear. Recent evidence also suggests that PINK1 plays a part in mitochondrial quality control via autophagy machinery, in collaboration with parkin (a cytosolic E3 ligase). In this review, we analyze the recent work published on PINK1 function, which can be a key factor in novel rational therapy for sporadic PD as well as *PINK1*-linked PD.

Clinical characteristics of PINK1-linked PD

Clinical features

The clinical features of *PINK1*-linked PD include parkinsonism associated with a good response to levodopa (the precursor to the dopamine), frequent occurrence of levodopa-induced dyskinesias, and infrequent occurrence of dystonia at onset, similar to those of sporadic PD. The only distinctive features are the earlier age of onset and slower progression [7]. The age of onset of *PINK1*-linked PD is around the early thirties [8,9], whereas that of sporadic PD is after the age of 60 years[1]. Unlike *parkin*-linked PD, hyperreflexia and sleep benefit are not common in *PINK1*-linked PD. However, some patients with *PINK1*-linked PD exhibit foot dystonia at onset and sleep benefit, mimicking those with *parkin*-linked PD. Others with *PINK1*-linked PD show atypical clinical features associated with psychiatric problems and dementia, both of which are rare in patients with *parkin*-linked PD.

Pathological features

As mentioned above, accumulation of Lewy bodies is the pathological hallmark of sporadic PD. Lewy bodies were also detected in the brain of a *PINK1*-linked PD patient with compound heterozygous mutations (c.1252_1488 del and c.1488 + 1G > A) [10], whereas they are absent in the brains of *parkin*-linked PD patients [11,12]. Other pathological changes seen in the PD patient with the compound heterozygous *PINK1*-mutations include neuronal loss in the substantia nigra pars compacta accompanied with astrocytic gliosis and moderate microgliosis. No apparent cell loss, Lewy bodies, or abnormal neurites are seen in the locus ceruleus. However, pathological examination has been reported in only one case of *PINK1*-linked PD, so further pathological studies are needed to determine the association between Lewy bodies and the pathogenesis of *PINK1*-linked PD.

PINK1

Molecular structure

The *PINK1* gene contains 8 exons spanning ~1.8 kilobases and encodes a 581–amino acid protein. The transcript is

Corresponding author: Hattori, N. (nhattori@juntendo.ac.jp).

0165-6147/$ – see front matter doi:10.1016/j.tips.2011.08.001 Trends in Pharmacological Sciences, October 2011, Vol. 32, No. 10

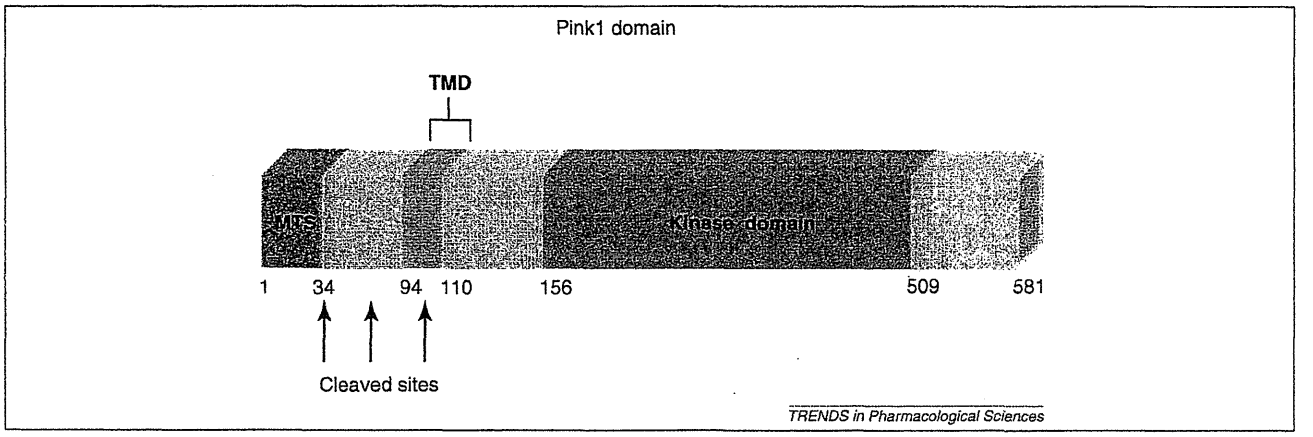

Figure 1. Putative functional domains and motifs of PINK1. Possible cleaved sites consist of the end of mitochondrial targeting sequence (MTS), sites between MTS and the transmembrane domain (TMD), and sites in the TMD.

ubiquitously expressed and predicted to encode an N-terminal 34–amino acid mitochondrial targeting sequence (MTS), a transmembrane domain (TMD) (residues 94–110) and a highly conserved protein kinase domain (residues 156–509) showing a high degree of homology to the serine/threonine kinases of the Ca^{2+}/calmodulin family [13] (Figure 1). It is important to understand the topology and subcellular distribution of PINK1 when considering PINK1 functions. PINK1 is a mitochondrial membrane integral protein whose kinase domain localizes in the outer mitochondrial membrane and is accessible from the cytoplasm. The TMD is crucial for anchoring PINK1 to the mitochondrial membrane and to ensure that the kinase domain faces the cytoplasm [14]. Subcellular fractionation shows that overexpressed PINK1 is localized in the mitochondria and cytoplasm [15], although the localization of endogenous PINK1 is not clear. This is because PINK1 is so rapidly turned over under basal conditions [16,17] that the expression level of PINK1 is very low and no antibodies against endogenous PINK1 are available. A chimeric protein consisting of a fluorescence protein fused to the N-terminus of PINK1 localizes to the mitochondria. Thus, the putative MTS of PINK1 is sufficient for its mitochondrial localization [18]. PINK1 translocated to the mitochondria by MTS is processed at several sites, such as 34 and/or 77 amino acids at the N-terminus and another site in the TMD. PINK1 mainly includes the full-length form (~63 kDa) and the cleaved form (~55 kDa) [15,18–20] (Figure 1).

Human genetics

PINK1 (PARK6) was identified in 2004 as a causative gene of autosomal recessive young-onset PD [13]. Since then, several mutations have been identified in PD patients in Europe and Japan [21]. With regard to the mode of inheritance (e.g. recessive form), loss of PINK1 function is proposed as the mechanism of *PINK1*-linked PD. The estimated prevalence of PINK1 mutations in different ethnicities is 1–8% of familial or young-onset PD [22]. Approximately 50 pathogenic mutations (missense mutations, genomic rearrangements, truncating mutations) have been identified in diverse populations. Most of the mutations are observed in the serine/threonine kinase domain, suggesting that loss of kinase activity plays a crucial part in the pathogenesis of *PINK1*-linked PD. Although the genotype–phenotype correlation has not been confirmed, the mean age at onset in patients with single heterozygous mutations is higher than that in patients with homozygous mutations [9,23]. Homozygous mutations in *PINK1* invariably cause *PINK1*-linked PD, whereas heterozygous mutations have been suggested to be a susceptibility factor for sporadic PD [24].

PINK1 function

Kinase activity

As mentioned above, PINK1 is a serine/threonine kinase protein. Several studies have reported that pathogenic mutations in PINK1, such as p.K219A, p.G309D, p.L347P, p.D362A, p.D384A, p.G386A, p.G409 V, p.E417G, are associated with reduced kinase activity [5,15,18,25]. Furthermore, the C-terminus of PINK1 regulates its kinase activity, although there is controversy over whether it up-regulates or down-regulates [18,25] activity [25]. Mutations in the PINK1 C-terminus cause early-onset parkinsonism [26]. Therefore, we have to consider the effect of the C-terminus on kinase activity to be significant. TNF receptor-associated protein 1 (TRAP1), a mitochondrial chaperone, has been identified as a PINK1 substrate. PINK1 might provide protection against oxidative stress-induced apoptosis by the phosphorylation of TRAP1 [5]. Another candidate substrate of PINK1 is parkin. The linker region of parkin is phosphorylated by PINK1, and parkin phosphorylated by PINK1 promotes its mitochondrial translocation [27]. The activity of parkin E3 ligase functions to catalyze the K63-linked polyubiquitination of IKKγ, which is a critical step in the cytoprotective signaling pathway that activates NF-κB, a ubiquitously expressed transcription of several pro-survival genes [18,28]. PINK1 is thought to modulate the phosphorylation status of another mitochondrial protein, Omi/HtrA2 (a gene product for *PARK13*), possibly through indirect mechanisms [6]. Rictor, a specific component of mammalian target of rapamycin complex 2 (mTORC2), is phosphorylated by overexpression of PINK1. Enhanced Akt through activation of mTORC2

provides cytoprotection [20,29]. These reports corroborate the fact that kinase activity has crucial roles in the pathogenesis of *PINK1*-linked PD.

Interaction with other PD-associated genes

PINK1-deficient *Drosophila* and *PINK1*-linked PD patients show very similar phenotypes, in contrast to flies and patients whose symptoms are caused by *parkin* mutations. Moreover, overexpression of parkin rescues the phenotype of *PINK1*-deficient *Drosophila*, but not *vice versa* [30,31]. However, Omi/HtrA2 is not an essential component of the PINK1/parkin pathway in *Drosophila* [32]. In cultured cells, PINK1 knockdown phenotypes are also rescued by overexpression of parkin, but not *vice versa* [33]. Parkin stabilizes PINK1 through direct interaction [34]. These results suggest that PINK1 functions upstream of parkin in a common pathway. Furthermore, parkin, PINK1, and DJ-1 form a ubiquitin E3 ligase complex that promotes the degradation of unfolded proteins [35]. In *Drosophila*, DJ-1 can rescue the consequences of PINK1 loss (except for infertility), but not the consequences of parkin loss. Furthermore, parkin cannot rescue DJ-1 loss, suggesting that DJ-1 may not be directly downstream of PINK1 [26,36]. In human neuroblastoma cells, parkin protects against the loss of DJ-1 and, although DJ-1 does not alter *PINK1*-deficient mitochondrial phenotypes, DJ-1 is active against rotenone-induced damage in the absence of PINK1 [27,37]. These findings indicate that DJ-1 works in parallel to the PINK1/parkin pathway to maintain mitochondrial function.

PINK1 knockdown causes proteasome dysfunction, accompanied by increased α-synuclein aggregation [38]. *PINK1*-deficient *Caenorhabditis elegans* exhibits a reduced length of mitochondrial cristae, increased sensitivity to paraquat (a herbicide which causes oxidative stress and parkinsonism) and defective axonal outgrowth of a pair of canal-associated neurons. In the absence of LRRK2, all these phenotypic aspects can be suppressed [39]. Furthermore, in *Drosophila*, overexpression of LRRK2 potentiates the bristle loss phenotype of PINK1 [40]. These results suggest that loss of LRRK2 suppresses the PINK1 phenotype. Taken together, evidence suggests that dysfunction of several causative gene products might contribute to the pathogenesis for PD through a common pathway (Figure 2).

Mitochondrial regulation

Mitochondrial function: In cultured cells, overexpression of PINK1 confers resistance to toxins against mitochondria such as staurosporine, 1-methyl-4-phenyl-1,2,3,6-tetrahydropyridine (MPTP), and rotenone, and PINK1 expression provides resistance to MPTP-induced dopaminergic neuronal loss in mice [4,41]. Consistent with these reports, reduction of PINK1 levels by RNA interference (RNAi) in cultured cells resulted in enhanced cell death in the presence of MPTP and rotenone [42]. In this regard, *PINK1*-deficient animal models and model-derived cells have provided important information on the endogenous function of PINK1. *PINK1*-deficient *Drosophila* showed degeneration of flight muscles, male sterility, and dopaminergic neuronal cells accompanied by mitochondrial abnormality, and shared phenotypic similarity with *parkin*-deficient *Drosophila* [30,31]. These models exhibit decreases in mitochondrial membrane potential ($\Delta\Psi m$), mitochondrial DNA, complex I, ATP, and an increased proportion of swollen mitochondria and susceptibility to apoptotic stimuli. Concomitant defects in synaptic function are also observed [43]. These results suggest that

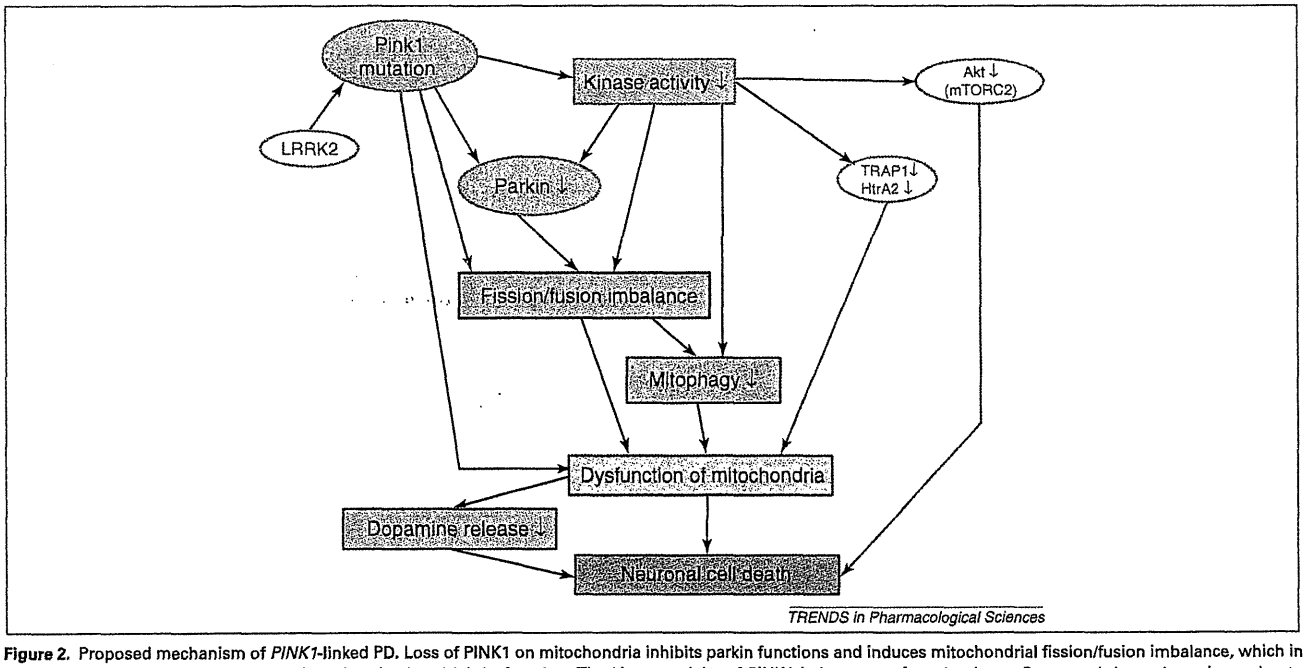

Figure 2. Proposed mechanism of *PINK1*-linked PD. Loss of PINK1 on mitochondria inhibits parkin functions and induces mitochondrial fission/fusion imbalance, which in turn causes impaired mitophagy, resulting in mitochondrial dysfunction. The kinase activity of PINK1 is important for mitophagy. Decreased dopamine release due to mitochondrial dysfunction induces neuronal cell death. Furthermore, TRAP1 and HtrA2 are not activated under reduced PINK1 kinase activity, leading to mitochondrial dysfunction. Reduced PINK1 kinase activity also results in failure of activation of Akt, leading to decreased cytoprotective function. LRRK2 exacerbates loss of PINK1.

loss of PINK1 can cause dopaminergic neuronal cell death due to functional defects in mitochondria.

In contrast, *PINK1*- and *parkin*-deficient mice do not exhibit major abnormalities, whereas absence of PINK1 causes several deficits, including: (i) reduced synaptic dopamine release and plasticity in the striatum [44]; (ii) impaired mitochondrial respiration in the striatum at 3–4 months of age and in the cerebral cortex at 2 years [45]; and (iii) progressive weight loss and selective reduction of locomotor activity for spontaneous movements in old age [46]. These findings indicate that the mitochondria in *PINK1*-deficient models are more vulnerable to aging. Primary cultured neurons derived from *PINK1*-deficient mice showed increased intracellular calcium levels and vulnerability, with subsequent excess production of reactive oxygen species (ROS), decreased glucose availability, loss of $\Delta\Psi m$ and defects of complex I, causing pathological opening of the mitochondrial permeability transition pore [47]. In *PINK1*-deficient mouse embryonic fibroblasts (MEFs), $\Delta\Psi m$ and cellular ATP levels are lower than in wild-type MEFs. However, mitochondrial proton leak (which reduces membrane potential in the absence of ATP synthesis) is not altered by loss of PINK1. Instead, low activity of the respiratory chain (which produces membrane potential oxidizing substrates using oxygen) has been observed [48]. These results suggest that decreased $\Delta\Psi m$ caused by loss of PINK1 is not due to proton leak, but to respiratory chain defects [39].

Similar to *parkin*-deficient mice, *PINK1*-deficient mice do not show prominent phenotypes. However, results from *PINK1*-deficient mice indicate that dysfunction of mitochondrial proteins (e.g. complex I) and aging are important in the pathogenesis of *PINK1*-linked PD as well as in sporadic PD.

Samples obtained from patients with hereditary PD can provide important information regarding the pathogenesis of PD. Skin fibroblasts of patients homozygous for the p.G309D *PINK1* mutation show: (i) a mild decrease in complex I activity and a trend of superoxide elevation [49]; (ii) fragmented mitochondrial morphology [33]; and (iii) low expression of parkin and selective vulnerability to proteasomal stress-triggered caspase activation [41,50].

In samples obtained from mice and PD patients, as well as from cultured cells, loss of PINK1 causes mitochondrial dysfunction and vulnerability to cell death.

Mitochondrial morphology: In mammalian cultured cells (with the exception of COS7 cells), PINK1 knockdown phenotype shows fragmented mitochondria [33,51]. In human neuroblastoma cells transduced with a PINK1 shRNA lentivirus, the activity of dynamin-related protein 1 (Drp1), which is controlled by phosphatase calcineurin, enhances the effects of PINK1 upon mitochondrial morphology [52]. In contrast, transgenic *Drosophila* with PINK1 promotes mitochondrial fission in dopaminergic neurons, whereas complete ablation of PINK1 leads to excessive fusion [53]. Fis1 (mitochondrial fission 1 protein) may act in-between PINK1 and Drp1 in controlling mitochondrial fission [53]. Heterozygous loss-of-function mutations of Drp1 are largely lethal in a *PINK1* or *parkin* mutant background. Conversely, the degeneration of flight muscle and mitochondrial morphological changes which result from mutations in *PINK1* and *parkin* are strongly suppressed by increasing the dosage of the Drp1 gene and by heterozygous loss-of-function mutations in OPA1 and Mfn2. In pseudopupil analyses, an eye phenotype associated with increased activity of the PINK1/parkin pathway is suppressed by perturbations that reduce mitochondrial fission but enhanced by perturbations that reduce mitochondrial fusion [54,55]. These results suggest that the PINK1/parkin pathway promotes mitochondrial fission, and that the loss of mitochondrial and tissue integrity in *PINK1* and *parkin* mutants is due to reduced mitochondrial fission in *Drosophila*. The cortical neurons of *PINK1*-deficient mice show reduced fission and increased aggregation of mitochondria only under stress [46]. Dopaminergic neuronal rat cells with a *PINK1* mutation (p.L347P) show mitochondrial fragmentation and dysfunction, which can be prevented by inhibitors of mitochondrial division [47,56].

There is controversy over whether PINK1 modulates mitochondrial fission or fusion. Fragmented mitochondria in *parkin* and/or *PINK1*-deficient *Drosophila* S2 cells are observed at day 2 after double-stranded RNA (dsRNA) treatment. At days 3 and 4 after dsRNA treatment, a dense network of fine thread-like mitochondria is observed. *PINK1*-deficient primary mouse hippocampal neurons show a decrease in the length of mitochondria and an increase in mitochondrial fragmentation. The mitochondrial phenotype observed in *parkin*- and *PINK1*-deficient cells can be rescued morphologically and functionally by increased expression of a dominant negative mutant of Drp1 [51]. Considering the discrepancy between cellular and fly models with low PINK1 expression, we might observe an acute manifestation of *parkin* or *PINK1* knockdown in cultured cells and the chronic phenotype influenced by compensatory effects in adult *Drosophila* (although the mitochondrial morphological change might be dependent upon cell lines). Otherwise, PINK1 might regulate and maintain a balance between fission and fusion depending upon certain conditions (e.g. phase, stress).

Mitochondrial fission and fusion are highly regulated processes that are critical for the maintenance of mitochondria (especially in neurons). Imbalance of mitochondrial fission and fusion machineries has increasingly been linked to neurodegeneration [57]. Based on this concept, PINK1 has a crucial role in the pathogenesis of PD.

Mitophagy: Recent studies have provided new insights about the PINK1/parkin pathway. It has been reported that parkin is translocated to depolarized mitochondria and that the parkin-labeled mitochondria are subsequently eliminated by autophagy (mitophagy) [58]. Several studies on this pathway were subsequently reported. Endogenous PINK1 is not detected under basal conditions because it is rapidly degraded [16]. However, reduction of $\Delta\Psi m$ induced by carbonyl cyanide *m*-chlorophenylhydrazone (CCCP), a mitochondrial uncoupler, results in gradual accumulation of endogenous PINK1 (full-length form) on mitochondria [17,59]. Interestingly, clearance of CCCP results in immediate disappearance of the accumulated endogenous PINK1 in the presence and absence of cycloheximide (an inhibitor of protein biosynthesis) by interfering with the translocation step of protein synthesis.

Likewise, CCCP treatment does not alter PINK1 mRNA levels [17]. These results suggest that PINK1 is stabilized by reduced $\Delta\Psi m$ and subsequently accumulates on depolarized mitochondria. By contrast, parkin is not translocated to the mitochondria in *PINK1*-deficient CCCP-treated MEFs, and subsequent mitochondrial clearance is also completely blocked, indicating that PINK1 is indispensable for parkin translocation to depolarized mitochondria. Parkin E3 ligase activity is suppressed under basal conditions, although the activity is increased in mitochondria with low $\Delta\Psi m$. PINK1 accumulation induces recruitment of parkin to the depolarized mitochondria, and subsequently the mitochondria are eliminated by mitophagy. These processes are inhibited by pathogenic mutants of PINK1 or parkin [16,17,59]. Furthermore, elimination of parkin-labeled mitochondria is blocked in *Atg5*- or *Atg7*-deficient MEFs [58,59]. Moreover, MTS, kinase activity of PINK1, and the linker domain of parkin are indispensable for PINK1/parkin-mediated mitophagy [17,52,59].

In cells with normal $\Delta\Psi m$, expression of PINK1 on the outer mitochondrial membrane or overexpression of PINK1 induces translocation of parkin to the mitochondria [60,61]. Furthermore, valinomycin- and hydrogen peroxide (H_2O_2)-induced stress result in mitochondrial localization of parkin in skin fibroblasts of healthy controls but not in those of PD patients with PINK1 mutations (p.Q456X) [56,62]. Valinomycin, but not H_2O_2, reduces $\Delta\Psi m$. Taken together, it seems that PINK1 expression on the mitochondria, rather than low $\Delta\Psi m$, is indispensable for parkin translocation to the mitochondria.

The mitochondrial inner membrane rhomboid protease presenilin-associated rhomboid-like protein (PARL) mediates cleavage of PINK1 in the TMD in a $\Delta\Psi m$-dependent manner. In the absence of PARL, full-length PINK1 accumulates on the outer mitochondrial membrane, where it recruits parkin to the impaired mitochondria. Thus, the role of PARL in the PINK1/parkin pathway appears to include facilitating the rapid degradation of PINK1 by mediating the cleavage of PINK1 [19,20,63].

PINK1/parkin-mediated mitophagy involves the formation of linkage-specific polyubiquitin chains (K27 and K63) and requires the ubiquitin-autophagy adaptor p62/SQSTM1. VDAC1 is a mitochondrial target of parkin-dependent K27 ubiquitination, and VDAC1 ubiquitination in neuronal cells is dependent upon functional parkin. Because VDAC1 is a component of the mitochondrial permeability transition pore (mPTP), which is involved in apoptosis, a parkin-dependent, timely mitophagic clearance may prevent the release of pro-apoptotic factors from damaged mitochondria under physiological conditions [58,64]. By contrast, p62 is reported to be necessary for mitochondrial aggregation but not mitophagy, and mitochondrial-associated proteins other than VDAC1 and VDAC3 are K63-polyubiquitinated in a parkin-dependent manner [65,66]. Another candidate parkin substrate on the mitochondria is mitofusin (MFN), which is involved in mitochondrial fusion. *Drosophila* Marf (a fly MFN ortholog), which is localized on the outer surface of mitochondria, is ubiquitinated by parkin and accumulates in *parkin* mutants [67,68]. Mammalian cells contain two types of MFN: MFN1 and MFN2. Treatment of cultured cells with CCCP results in ubiquitination of MFN1 and MFN2 in a PINK1/parkin-dependent manner [63,69]. Moreover, parkin-ubiquitinated MFN1 and MFN2 are degraded by the proteasome. The hexametric AAA-type ATPase, p97, is required downstream of PINK1 and parkin to promote the proteasomal turnover of ubiquitinated MFN. Parkin-promoted MFN degradation prevents refusion of damaged mitochondria with healthy mitochondria [64,70]. Fission followed by selective fusion segregates dysfunctional mitochondria and permits their removal by autophagy [71]. These reports suggest that mitochondrial fission may be a key factor in PINK1/parkin-mediated mitophagy. However, there is controversy over the substrates of parkin, making further investigations necessary.

PINK1/parkin-mediated mitophagy model

Based on the collective results of the studies mentioned above, we propose the model illustrated in Figure 3 for PINK1/parkin-mediated mitophagy. PINK1 accumulated on the mitochondrial outer membrane due to the low $\Delta\Psi m$ or certain mitochondrial insults recruit parkin to the mitochondria. Parkin E3 ligase activity is subsequently activated and ubiquitinates MFN on the mitochondrial outer membrane. Ubiquitinated MFN assembles p97 and the complex is degraded by proteasome. Mitochondria lacking MFN, which cannot fuse with other healthy mitochondria, can be a target for mitophagy. The model advances our understanding of the pathogenic process of PD and the role of the direct associations between parkin and mitochondria, as well as between the PINK1/parkin pathway and autophagy. Mitochondrial dysfunction is also considered to be one of the main causes of the sporadic form of PD, and impaired autophagy leads to neurodegenerative diseases such as PD. However, to fully understand the molecular mechanisms of this pathway, further details are needed. For example, how does PINK1 recruit parkin to the damaged mitochondria? What is the mechanism responsible for parkin activation in the mitochondria? There is controversy over whether PINK1 phosphorylates parkin in this pathway [16,17,27,28,61,66]. PINK1 kinase activity is essential for parkin translocation to mitochondria [17,59]. Therefore, it is a feasible and attractive hypothesis that parkin is directly phosphorylated by PINK1. However, further investigations are needed.

Other candidate PINK1 substrates that recruit parkin or function as parkin receptors on the outer mitochondrial membrane also need to be investigated. In yeast, Atg32 (which has no known metazoan homolog) is identified as an outer mitochondrial membrane protein necessary for mitophagy [72,73], and contains a conserved WXXI/L/V motif for interaction with Atg8. Recent studies reported that another outer mitochondrial membrane protein, Nix (which has no yeast homolog and contains a WXXL-like motif), is crucial for PINK1/parkin-mediated mitophagy [68,74]. Does endogenous parkin contribute to mitophagy? Most reports on this pathway are conducted by overexpressing parkin. It remains unclear at this stage whether parkin deficiency or parkin partial knockdown down-regulates mitophagy. Furthermore, there is no information on whether $\Delta\Psi m$ of the brain is decreased in patients with

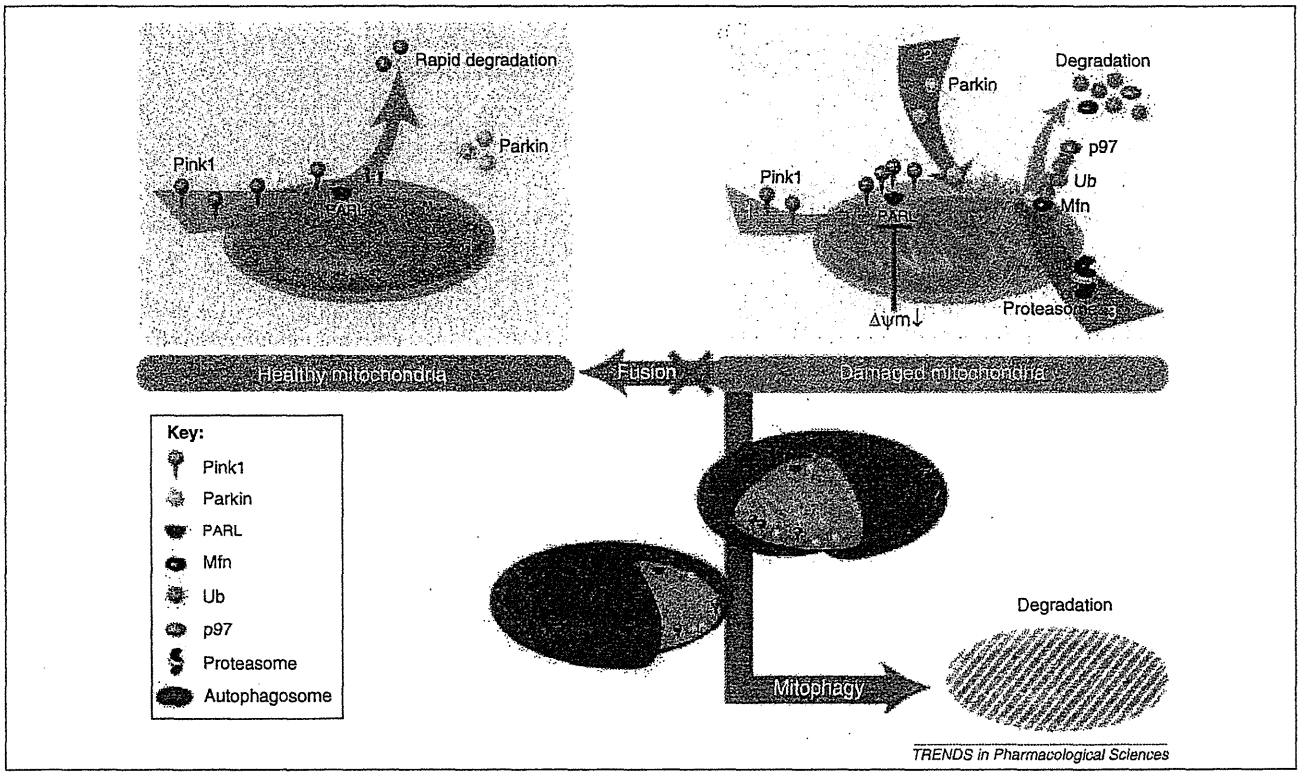

Figure 3. Proposed model of PINK1/parkin-mediated mitophagy. PINK1 on mitochondria is processed by PARL, which localizes in the mitochondrial inner membrane under basal conditions. The processed PINK1 is rapidly degraded by the proteasome. In the presence of a low membrane potential or certain insults to the mitochondria, PINK1 accumulates in the mitochondrial outer membrane. This results in translocation of parkin to the damaged mitochondria and subsequent activation of parkin-E3 ligase. Activated parkin ubiquitinates mitofusin (MFN) on the mitochondrial outer membrane. This leads to the assembly of p97 on ubiquitinated MFN and proteasomal degradation. Mitochondria lacking MFN cannot fuse with other healthy mitochondria and become a target for mitophagy.

sporadic PD. As mentioned above, *PINK1*-deficient mice and MEFs as well as PINK1 knockdown cells show decreased $\Delta\Psi m$. However, skin fibroblasts derived from neither the nonsense (p.Q456X) nor the missense (p.V170G) mutation show significantly low $\Delta\Psi m$ [75]. There is no model of CCCP-induced human parkinsonism, unlike with MPTP-and rotenone-induced parkinsonism. In this regard, there is no evidence for translocation of parkin to mitochondria in cells treated with MPTP or rotenone. CCCP treatment does not reflect a human physiological condition. Therefore, there is a limitation in discussing the pathogenesis of PD using models based on CCCP treatment.

Is there any association between PINK1/parkin-mediated mitophagy and α-synuclein? As discussed above, α-synuclein is a major component of Lewy bodies (the hallmark of sporadic PD) and is considered to be a key protein in the pathogenesis of sporadic PD. There is no direct association between PINK1/parkin-mediated mitophagy and α-synuclein, although wild-type and mutants of α-synuclein are degraded by chaperone-mediated autophagy and macroautophagy, respectively [76,77]. Studies demonstrated that α-synuclein inhibits autophagy [71,78], and that inhibition of mitochondrial fusion by α-synuclein is rescued by PINK1 and parkin [72,73,79]. To develop a novel therapeutic strategy for sporadic PD as well as *PINK1*- and *parkin*-linked PD, it is necessary to investigate the relationship between aggregation of α-synuclein and dysfunction of PINK1/parkin-mediated mitophagy.

Concluding remarks

PD is a progressive neurodegenerative disease for which the frequency increases with age. As 'developing nations' face rapidly aging populations, the prevalence of PD is expected to rise. PD patients in the advanced stage require great support from families and the medical community. However, curative therapies to suppress the progression are lacking. Therefore, it is important to elucidate the pathogenesis and establish novel and rational treatments. PINK1 provides valuable clues regarding the molecular pathogenesis of PD because the pathomechanism for sporadic PD probably has certain common pathways with that of *PINK1*-linked PD. Based on the available information on PINK1, we propose the model shown in Figure 2 for the mechanisms involved in the development of *PINK1*-linked PD. PINK1 mainly protects the mitochondria via mitophagy with parkin, and may subsequently suppress neuronal cell death due to reduced dopamine release. However, PINK1 may have a cytoprotective function by activating Akt in the cytoplasm. We expect that a compound which inhibits this pathway could be established as a novel treatment for not only *PINK1*-linked PD but also sporadic PD. In particular, PINK1/parkin-mediated mitophagy (i.e. mitochondrial quality control via autophagic machinery that includes the combination of PINK1 and parkin) could be viewed as the foundation for the design of novel therapies for PD, although several issues remain unresolved. If we could determine the precise mechanism of mitophagy which eliminates abnormal mitochondria, we